HELSINGIN YLIOPISTO
HELSINGFORS UNIVERSITET
UNIVERSITY OF HELSINKI

Master's Degree Programme in Biotechnology (MBIOT)
Faculty of Biological and Environmental Sciences
University of Helsinki
Finland
2020

Key inflammatory modulation effects of porous silicon nanoparticles with different surface chemistries

Master’s thesis

by

Khalil Elbadri

Supervisor: Prof. Hélder A. Santos
Co-supervisor: Dr. Zehua Liu

Tiedekunta – Fakultet – Faculty **Faculty of Biological and Environmental Sciences**	Koulutusohjelma – Utbildingsprogram – Degree Programme **Master's Degree Programme in Biotechnology (MBIOT)**

Tekijä – Författare – Author
Khalil Elbadri

Työn nimi – Arbetets titel – Title
Key inflammatory modulation effects of porous silicon nanoparticles with different surface chemistries

Oppiaine/Opintosuunta – Läroämne/Studieinriktning – Subject/Study track
Molecular Biotechnology (MBIOT)

Työn laji – Arbetets art – Level **Master's Degree**	Aika – Datum – Month and year **April 2020**	Sivumäärä – Sidoantal – Number of pages **75**

Tiivistelmä – Referat – Abstract

An increased attention has been drawn towards porous silicon (PSi) based materials for biomedical applications, due to their promising features demonstrated through several scientific studies. Here, we further investigated the biological responses of PSi nanoparticles (NPs) with different surface chemistries, including immunomodulatory effects, inflammation mitigation and biocompatibility. In this collaborative study, the PSi NPs were investigated both *in vitro* and *in vivo*, using different molecular biology and biochemistry techniques, *e.g.*, qPCR, ELISA, cell sorting and cell viability assays. Our results showed the capabilities of these PSi NPs to relieve the inflammatory conditions, whereas significant decrease was recorded of pro-inflammatory cytokines: TNF-α, IL-1β and IL-6. Likewise, these PSi NPs revealed a considerable consumption aptitude of pro-inflammatory reactive oxygen species molecules. Administrating PSi NPs in an acute liver inflammation (ALI) model, showed no conspicuous influence on cellular viability. Thus, the outcome of this study demonstrates the potential biocompatibility of PSi nanomaterials, in addition to their outstanding features as potential candidates for further incorporating in ALI applications.

Avainsanat – Nyckelord – Keywords
Porous silicon, inflammation, nanotechnology, nanoparticles, molecular biology, biotechnology, liver, surface chemistry, cell viability, reactive oxygen species, ROS

Ohjaaja tai ohjaajat – Handledare – Supervisor or supervisors
Supervisor: Prof. Hélder A. Santos
Co-supervisor: Dr. Zehua Liu

Säilytyspaikka – Förvaringställe – Where deposited

Muita tietoja – Övriga uppgifter – Additional information

Abstract

An increased attention has been drawn towards porous silicon (PSi) based materials for biomedical applications, due to their promising features demonstrated through several scientific studies. Here, we further investigated the biological responses of PSi nanoparticles (NPs) with different surface chemistries, including immunomodulatory effects, inflammation mitigation and biocompatibility. In this collaborative study, the PSi NPs were investigated both *in vitro* and *in vivo*, using different molecular biology and biochemistry techniques, *e.g.*, qPCR, ELISA, cell sorting and cell viability assays. Our results showed the capabilities of these PSi NPs to relieve the inflammatory conditions, whereas significant decrease was recorded of pro-inflammatory cytokines: TNF-α, IL-1β and IL-6. Likewise, these PSi NPs revealed a considerable consumption aptitude of pro-inflammatory reactive oxygen species molecules. Administrating PSi NPs in an acute liver inflammation (ALI) model, showed no conspicuous influence on cellular viability. Thus, the outcome of this study demonstrates the potential biocompatibility of PSi nanomaterials, in addition to their outstanding features as potential candidates for further incorporating in ALI applications.

Acknowledgments

"Almighty God, Exalted are You; we have no knowledge except what You have taught us. Indeed, it is You who is the All-Knowing, the All-Wise"

"The absolute acknowledgement goes to the strongest and very first person I have ever known since the first time I opened my eyes, my mother. I owe you a great gratitude, which can never be fulfilled."

This thesis work was conducted as part of my MSc studies in the University of Helsinki; thus, I would like to express my great thankfulness for having such an amazing opportunity, which has enriched my knowledge and gave me the chance to widen my horizons. I believe it is a magnificent step in my scientific career.

A special acknowledgment has to be presented to Prof. Hélder A. Santos, who supervised and hosted me in his research group, and who has always been an inspiring man, representing a real example of successful role model with impressive knowledge, dedication and remarkable attitude. Without him, this work could have not been done. Likewise, I would like to thank the amazing members of Santos' Lab, who helped me a lot during my thesis, especially my co-supervisor Dr. Zehua Liu and the best lab technician Alexandra Correia.

Sincere appreciation and gratitude to all my former teachers who enlightened my way and provided me with all needed support along my studying journey. However, it is impossible to include every one of them here, I specially thank Assoc. Prof. Mahmoud Ibrahim, Assoc. Prof. Abdelnasser Hosny Alshorafa and Dr. Sherine Abdel Salam.

Ultimately, I would like to express my immense gratitude to every amazing person in my life who always support me, primarily my family; my brother Ahmed Elbadri, my brother in Law Ibrahim Uzunöz, my sister Fatima Elbadri, my life-journey companion Virginia, and my dear friends; especially Hussein Alburkat and Abdallah Ahmed.

For the dear friends, family members and teachers who are reading this and might think I have forgotten to mention them: "You are all in my heart even if your names are not on this paper".

List of abbreviations and symbols

$-NH_2$	Amines
°C	Celsius degree
ABC	Accelerated blood clearance
ALI	Acute liver inflammation
ALP	Alkaline phosphatase
ALT	Alanine aminotransferase
APAP	Acetaminophen
APCs	Antigen presenting cells
APM	Poly(methyl vinyl ether-alt-maleic acid) conjugated apstcpsi
APSTCPSi	(3-Aminopropyl)triethoxysilane functionalized thcpsi
AST	Aspartate aminotransferase
ATP	Adenosine triphosphate
CARPA	Complement activation-related pseudoallergy
CCL2	Chemokine (C-C motif) ligand 2
CD80,83, 86	Cluster of differentiation 80, 83, 86
cDNA	Complementary deoxyribonucleic acid
cm	Centimeter
CNTs	Carbon nanotubes
CXCL1	C-X-C motif chemokine ligand 1
DCF	Dichlorofluorescein
DCF-DA	2´,7´-Dichlorodihydrofluorescein diacetate
DCs	Derived dendritic cells
DLS	Dynamic light scattering
DMSO	Dimethyl sulfoxide
ELISA	Enzyme-linked immunosorbent assay
EtOH	Ethyl alcohol
FACS	Fluorescence-activated cell sorting
FBS	Fetal bovine serum
FTIR	Fourier-transform infrared spectroscopy
GAPDH	Glyceraldehyde-3-phosphate dehydrogenase
gDNA	Genomic deoxyribonucleic acid
GRA	Granulocytes
GSH	Glutathione
H	Hour
HCC	Hepatocellular carcinoma
HIV	Human immunodeficiency viruses
HLA-DR	Human leukocyte antigen-D related
HR-TEM	High resolution transmission electron microscope
IFN-γ	Interferon gamma cytokine
IL-12	Interleukin-12
IL-1β	Interleukin 1 beta
IL-6	Interleukin 6
IU	International unit
JRC	Joint research centre
Kg	Kilogram
LDH	Lactate dehydrogenase

LPS	Lipopolysaccharide
LYM	Lymphocytes
m	Meter
M	Molar concentration
MDDCs	Untreated human monocyte-derived dendritic cells
MDEM	Dulbecco's modified eagle medium
mg	Milligram
min	Minute
mL	Milliliter
mM	Millimolar
MON	Monocytes
MP-AES	Microwave plasma atomic emission spectroscopy
MPS	Mononuclear phagocyte system
mRNA	Messenger RNA Ribonucleic acid
mV	Millivolt
NAFLD	Nonalcoholic fatty liver disease
NaOH	Sodium hydroxide
NIH	National Institutes of Health
NIR	Near-infrared
nm	Nanometer
nm	Nanometer
NPs	Nanoparticles
ns	Nanosecond
p188	Poloxamer 188
PBMCs	Peripheral blood mononuclear cells
PBS	Phosphate-buffered saline
PC	Protein corona
PDTs	Photodynamic therapies
pg	Picogram
PLGA	Polylactic-*co*-glycolic acid
PSA	Prostate specific antigen
PSi	Porous silicon
PSi ML_{50}	The time required for half of psi mass to degrade
PTT	Photothermal therapy
PVA	Polyvinyl alcohol
QDs	Quantum dots
qPCR	Real-time polymerase chain reaction
RNA	Ribonucleic acid
ROS	Reactive oxygen species
RPM	Revolutions per minute
Si	Silicon
SIN-1	3-Morpholinosydnonimine N-ethylcarbamide
SPIONs	Superparamagnetic iron oxide nps
SPR	Surface plasmon resonance
TCPSi	Thermally carbonized PSi
TEM	Transmission electron microscopy
Th1	T helper type 1 cells
THCPSi	Thermally hydrocarbonized PSi
TNF-α	Tumor necrosis factor alpha
TOPSi	Thermally oxidized PSi

UnP	Polyethyleneimine conjugated UnTHCPSi
UnTHCPSi	Undecylenic acid functionalized THCPSi
VA	Province of Varese, Italy
WBCs	White blood cells
WCA	Wetting contact angle
μg	Microgram
μl	Microliter
μM	Micromolar
δ-potential	Zeta potential

*Part conducted by our collaborators from Xiamen University, China:

Yunzhan Li, Zehua Liu, Li Li, Wenhua Lian, Yaohui He, Elbadry Khalil, Ermei Mäkilä, Wenzhong Zhang, Giulia Torrieri, Xueyan Liu, Jingyi Su, Yuanming Xiu, Flavia Fontana, Jarno Salonen, Jouni Hirvonen, Wen Liu, Hongbo Zhang, Hélder A. Santos*, and Xianming Deng**

Tandem-Mass-Tag based proteomic analysis facilitates analyzing critical factors of porous silicon nanoparticles in determining their biological responses under pathological condition

Table of Contents

1. Introduction

Nanotechnology can be defined as an efficient approach to control and manipulate materials at a nanoscale, whereas it has been found that the matter tends to exhibit different properties at scale of 1 to 100 nanometers, namely "nanomaterial". Nanomaterials are identified as particles having at least one dimension of ≤ 100 nm. In **Figure 1** [1], this size range is exhibited comparing to other different objects.

There are several physicochemical characteristics that favor nanomaterials over macro materials, for example, high surface-to-volume ratio that exponentially escalate the chemical reactivity of the nanomaterial in spite of their small volume, and the enormous surface area of these nanomaterials can be functionalized with different small molecules, metal ions, polymers and surfactants [2]. Owing to the nanoscale size and high surface area, these materials exhibit exceptional chemical and physical features, which make them suitable agents for developing expedient nanodevices that can be used in several biomedical, biological, physical and chemical applications.

For instance, nanoparticles (NPs) have demonstrated an exceptional ability to deliver drugs within ideal dosage, leading to more efficient therapeutic effect and less side-effects [3]. Furthermore, due to their optical properties, nanoparticles are being employed in imaging techniques for visualizing cellular and other biological specimens [4]. Also, many of semiconductor and metallic NPs exhibit promising features for cancer diagnosis and treatment depending on their surface plasmon resonance (SPR) enhanced light scattering and absorption. Au NPs are strong example of this, whereas, they are able to transform the absorbed light into confined heat that can be employed in selective laser photothermal therapy of cancer. Likewise, conjugation of Au NPs ligands precisely targeted to biomarkers on cancer cells, allowing for molecular-specific imagining and identification of cancer cells [5].

NPs also possess an antineoplastic effect that is exploited to inhibit tumor growth, as shown by Chen *et al.* [6], using multihydroxylated $[Gd@C_{82}(OH)_{22}]_n$ NPs that showed potential efficacy and minor toxicity. NPs are involved in many other sectors, including water disinfecting, textiles and food packing, especially owing to the antimicrobial

features of inorganic NPs comparing to organic compounds, which were found to be more toxic to the biological entities [7]. Similarly, Ag NPs are being used in wound bondages, catheters and other various products due to their antimicrobial properties [8]. Other NPs also are known for their antibacterial activities, including; TiO, ZnO, $BiVO_4$, Cu and Ni NPs, thus they are utilized for similar applications [9-12].

In other industries, NPs are also of high demand, because they can exhibit the potential catalytic properties. Thus they are introduced, for example, to accelerate some oxidation-reduction processes of some pollutants [13].

Due to these unusual characteristics, NPs are considered an essential tool of high demand in nanotechnology industry in addition to attract a great attention in scientific research in many sectors, including biomedicine, cosmetics, bioremediation, material sciences, electronics and food packing [14, 15]. Nowadays, there are more than 1500 nanotechnology-based products in the market, widely distributed among different fields, starting from toilets slates and hydrophobic self-cleaning surfaces to strengthened tires containing carbon nanotubes [16].

1.1. Brief history

Although nanotechnology is one of the leading technologies in the current age, it is not a latter-day innovation. Nanomaterials have been used since very long time ago [17]. The Lycurgus Cup from the 4^{th} century is an example of this early technology, which has been found to contain NPs of Ag and Au reflecting the light, giving the cup green color when lit from outside, and red color when lit from inside it looks red, as shown in **Figures 1B and 1C** [18].

Nevertheless, in the present time the nanotechnology term and the microscopic instrumentation were first presented in 1959 by the Nobel-winning physicist Richard Feynman, whereas he mentioned "*There's plenty of room at the bottom*" in his speech in California Institute of Technology. In his talk, Feynman cited a friend's suggestion: "(Albert R. Hibbs) *suggests a very interesting possibility for relatively small machines, saying", although it is a very wild idea, it would be interesting in surgery if you could swallow the surgeon. You put the mechanical surgeon inside the blood vessel, and it goes*

into the heart and "looks" around. (Of course, the information has to be fed out.) It finds out which valve is the faulty one and takes a little knife and slices it out. Other small machines might be permanently incorporated in the body to assist some inadequately-functioning organ." [19].

Later in 1986, the notion of cell repair machines has been proposed by Eric Drexler, in his book "*Engines of Creation*". He suggested these machines to efficiently and precisely repair the cellular damage within different levels, starting from the cellular structures and organelles to the DNA level. Later in 1996, dazzling array of conceptual diamondoid nanomedical components and nanorobots was emphasized by Robert Freitas in his first book of "*Nanomedicine*" series [16]. Since then the nanoscale functionalized particles have been enormously spreading around.

1.2. Nanomaterials in medicine

Nanotechnology principles are vastly applied in medicine, which created what's called "nanomedicine" field, referred by National Institutes of Health (NIH) [20]. In nanomedicine, diseases are handled at molecular and cellular levels, which makes it more manageable to trace where and how diseases originate. For instance, there are intensive investigations on the therapies that can manipulate the patients' own genes or modify some signaling pathways involved in diseases, towards finding an efficient treatment. Thus, in the near future researchers may be able to exhibit the whole DNA strands and execute some necessary repairing modifications through, for example, some nanorobots able to perform inside the cellular environment. Another interesting example still under development, is the *in-situ* nano-factories, which are composed of self-assembly components designed to be able to build the protein-based drugs at the targeted site, rather than the complicated delivery process during which the drug is usually decomposed by the body mechanisms.

Currently, there are many developed nanotechnologies already available, such as Au nanoshells, which are used within cancer therapy and bioimaging, and superparamagnetic iron oxide NPs (SPIONs), which are used to trace and damage cancer cells thermally, avoiding damaging the surrounding healthy cells "hyperthermia". Another interesting invention is the hollow nanocarriers, *e.g.*, liposomes which can be employed as carriers

to deliver anticancer drugs and other medication to the targeted diseased cells [16]. All of these technologies are proving nanomedicine as a promising alternative for the ordinary medical approaches, *e.g.*, chemotherapeutic medications that are considered toxic regarding to their unpleasant side effects.

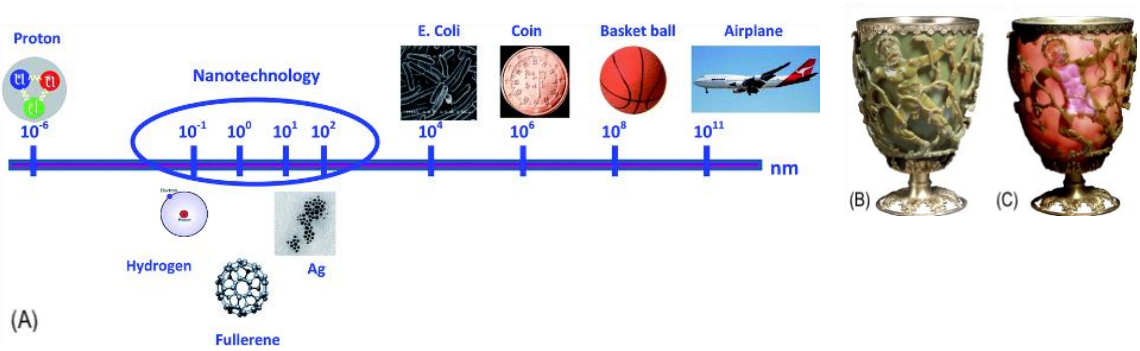

Figure 1:

(A) Size range of nanoparticles (10^{-1}–10^{2} nm) comparing to other objects.

(B-C) The Lycurgus Cup from the 4th century is an early nanotechnology-based example, which has been found to contain nanoparticles of Ag and Au. The pictures exhibit the fascinating phenomena about this Lycurgus cup, caused by the lights reflection manner, whereas, the cup appears green when is lit from outside **(B)**, while it looks red when it is lit from inside **(C)** [18].

*(Reference: López-Serrano, A., et al., Nanoparticles: a global vision. Characterization, separation, and quantification methods. Potential environmental and health impact. Analytical Methods, 2014. **6**(1): p. 38-56.)*

1.3. Classification of NPs and their potential biomedical applications

Several nanomaterials have been utilized for decades, *e.g.*, in glass crafting, and paintings, on the other hand, there are many other new discovered nanomaterials involved in variant fields, *e.g.*, in cosmetics, sports products and pyrotechnics (fireworks chemistry) [21]. Furthermore, there are also other applications under research, *e.g.*, medical implants, drug delivery, biodetectors, solar cells and fuel cell [22, 23].

The last decade has witnessed a hug increase in nanotechnology products **(Figure 2a)** [1]. However, it is worth mentioning that these products are mainly targeting health and fitness issues (**Figure 2b**) [1]. Nevertheless, NPs have been employed for many other applications, *e.g.*, environmental: bioremediation; accelerating the growth of some plants, and industrial: heat transfer; food manufacturing; personal care products; construction

supplies. However, in this study, we mainly discuss the biomedical applications of nanotechnology [1].

NPs are widely utilized within various biological applications, for example, biological markers due to their protein-like size range and their fluorescence features, *e.g.*, quantum dots. Furthermore, NPs compose the core of several nano-biomaterials are capable of interacting with biological objects within non-covalent interactions. Considerably, the approaches applied to build this nano-biomaterials are determined by the properties of those NPs, *e.g.*, their nature, biocompatibility, shape recognition, antigen detection, fluorescence monitoring [1, 24].

There are other microbiology related applications since NPs can be employed to detect bacterial existence, for example, CdS NP tracers are used through conjugating with specific bacteria to form a combination that permits DNA hybridization detection within immunological assays [24, 25]. Drug and gene delivery are other fields where NPs are also being employed. Incorporating drugs and genes within NPs provides protection against degradation and increase the cellular uptake [26, 27]. NPs are also used for protein ultrasensitive electrochemical detection, through nano-sizes biosensors, possessing significant versatility in addition to distinctive electrochemical features [28].

Likewise, quantum dots NPs are employed for fast and sensitive recognition of prostate specific antigen (PSA) within human serum with detection threshold of 20 pg/mL [29]. Additionally, DNA structure can be projected through establishing DNA conjugates, utilizing the distinctive optical and electronic features of those quantum dots NPs. Thus, these Au NPs are capable of differentiating between target-free and target-bound oligonucleotides through SPR [30], or alternatively, they are able to identify the target-responsive structural variations of DNA [31]. Also, NPs were found to be useful for microbial examining and detection, which may replace the *in vitro* and *in vivo* identifying of the target molecules. Therefore, sensors made of iron oxide have demonstrated significant sensitivity towards quantification of certain biomolecules within cell lysates and tissue extracts [32].

Currently, markets have witnessed a remarkable growth of using NPs for medical applications, *e.g.*, diagnosis, drug delivery and imaging [33]. This is a result of a continuous research and development of micro- and nano-technology, which have introduced remarkable amount of new and cutting-edge techniques for either synthesis or functionalization of these nanomaterials.

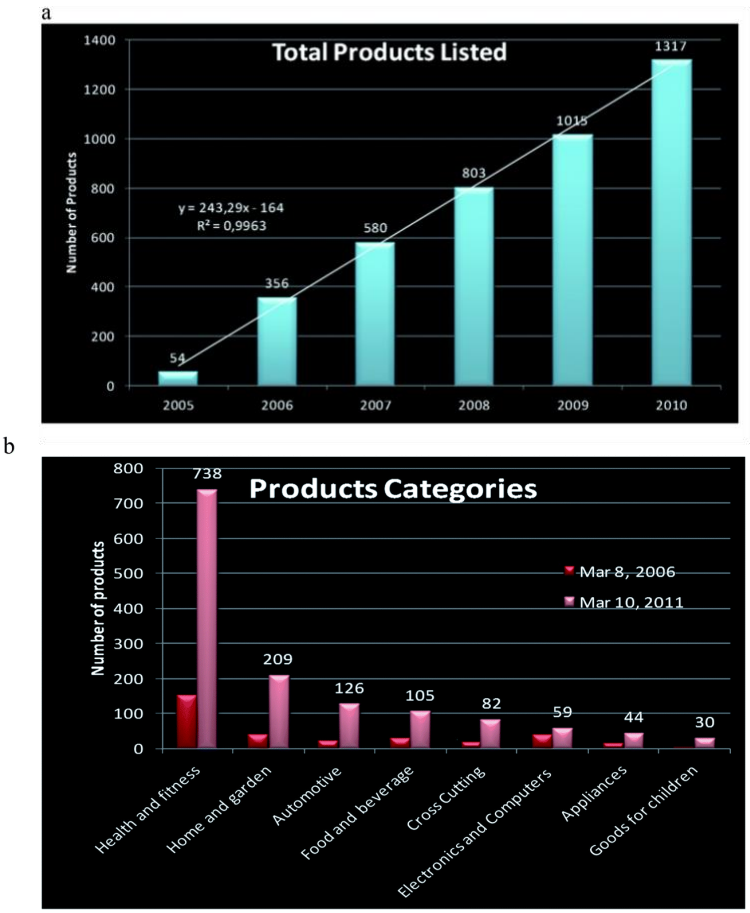

Figure 2: Products based on nanotechnology and the continuous growth over the last few years, whereas by 2010, nanotechnology-based products were estimated about 1300 **(a)**, and main categories of these nanotech products are demonstrated in figure **(b)** showing a huge great in health and fitness sector.

Reference:
http://www.nanotechproyect.org/inventories/consumer.

NPs can be categorized on variant considerations, *e.g.*, the origin (natural or anthropogenic), chemical structure (organic or inorganic), size, form and surface features, in addition to their applications.

1.3.1. Nanoparticles classified according to the chemical structure

1.3.1.1. Carbon-based nanomaterials

This category of nanomaterials is composed of pure carbon and it is categorized in two main sets: **1. Fullerene**: which is mainly a particle comprised of 60 carbon atoms at least; and **2. carbo nanotubes** (CNTs).

The most popular form of Fullerene is C-60, also called "buckminsterfullerene", and it is spherical carbon molecule in which the atoms are usually organized in truncated icosahedron construct [34]. Nevertheless, there are other less stable fullerene structures, *e.g.*, C_{70}, C_{76}, C_{78}, and C_{80} (**Figure 3a**) [35], which are utilized in different medical approaches. For instance, fullerenes have been found to possess an antiviral effect, in addition to their ability to penetrate and create connections in the catalytic sites of some enzymes. Thus, fullerenes were able to inhibit an HIV protease, which is critical for the survival of the virus. This reaction has been explained owing to the strong van der Waals interaction between the fullerene and the hollow surface of the enzyme [36].

CNTs occur in different types with different characteristics, fabricated in diverse techniques. Owing to their advantageous electrical, chemical and mechanical features they are of high demand in many fields, including medicine and biochemical industries [37]. CNTs can be used in eliminating many elements, for instance, pathogens, some natural organic substances and cyanobacterial toxins from water because of their extreme adsorption capability. CNTs have fibrous structure and huge external surface area (**Figure 3b**) [38], which is simply accessible by biological compounds/toxins [39].

1.3.1.2. Metal oxide NPs

This category of NPs comprises various transient metal oxides, *e.g.*, ZnO, TiO_2, CuO and SiO_2. Due to the special features of this elements, in addition to the remarkable reactivity feature of NPs, these NPs are used in many diverse industries, as catalysts and in medicine [40, 41]. For example, iron oxide NPs are commonly employed within many *in vivo* approaches due to their magnificent superparamagnetic features, *e.g.*, tissue repair, immunoassays, drug delivery, magnetic resonance imaging contrast enhancement and

detoxification of biological fluids [42]. Likewise, silicon (Si) NPs are important group in this category and they are utilized in various biomedical approaches, *e.g.*, drug delivery. However, we will discuss their properties later in this thesis.

1.3.1.3. Quantum dots (QDs)

These particles are auto-fluorescent semiconductors nanocrystals that are vastly used in *in vivo* imaging [24, 43-45], owing to their quantum incarceration feature. Moreover, QDs exhibit an interesting optical feature, for instance, sharp and symmetrical emission spectra, high photo steadiness and extreme quantum revenue. The most common structures of these QDs are binary metal complexes, *e.g.*, CdS, CdZn and CdSe, which are extensively applied in biological labelling within many sorts of animal cells. However, there are other forms of QDs created by amalgamation, for example, CdSe-ZnS core-shell nanocrystals, which are used as bioactive fluorescent probes for imaging, sensing, immunoassays and else diagnostic approaches.

1.3.1.4. Elemental metallic NPs

This group of NPs comprises inorganic NPs that are primarily constituted of noble elements, *e.g.*, Au and Ag, combined with other transition metals, *e.g.*, Fe and Zn. These particles are involved in many applications, such as, bioremediation and biomolecules detection. Ag NPs possess an exceptional antimicrobial feature, whereas the close contact between the silver nuclei and the cell wall, cause its interruption [46-49]. Also, gold NPs have lately acquired a big importance due to their conjugation possibility with the biomolecules across their function groups and act chemically as an anchor and element markers, thus they are widely used as element tags in proteomics [50].

1.3.1.5. Organic polymers

These are composed of organic polymers that are extremely stable upon contact with biological fluids. Thus, their polymeric features are of high potential for pharmaceutical purpose, *e.g.*, controlled and sustainable drug release. It has been shown in previous neurological studies that some of these biodegradable polymerics materials with specific surface adjustment were capable of delivering drug beyond the blood brain barrier in

favor of diagnostic and therapeutic approaches [51]. Additionally, due to the high capacity they have shown, upon modifying or imprinting, they are being applied to recognize and bind to targeted chemical compounds, in addition to some analytical approaches, *e.g.*, solid phase extraction and clinical analysis. For example, artificial antibodies with high selectivity and sensitivity were developed by molecularly imprinted polymeric NPs synthesized for human rhinovirus immunoglobulins [52]. **Table 1** summarizes the different types NPs and their common biomedical applications.

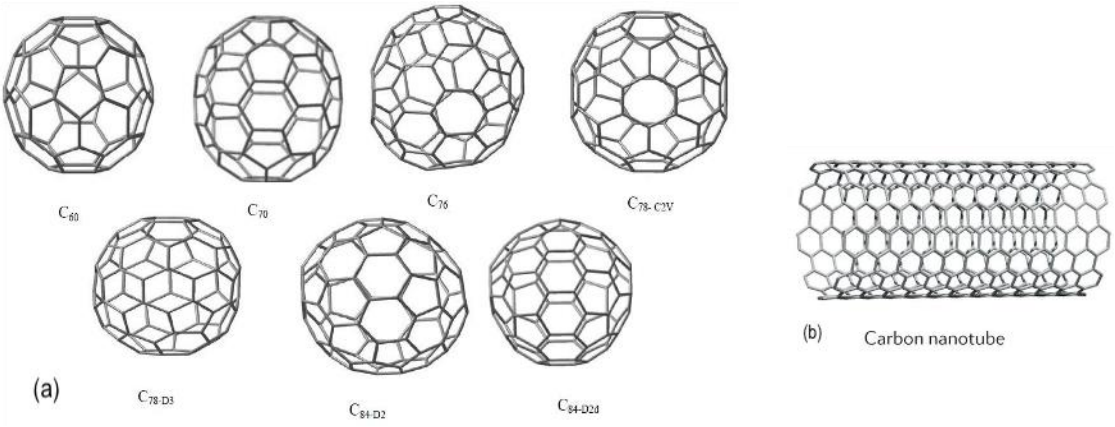

Figure 3: (a) Different forms of Carbon-based nanomaterials, including Fullerenes (C_{60}, C_{70}, C_{76}, $C_{78\text{-}C2V}$, $C_{78\text{-}D3}$, $C_{84\text{-}D2}$ and $C_{84\text{-}D2d}$, in addition to **(b)** nanotube form.

*(Reference for this model: (a) Louazri, L., et al., Study of the Effect of Substitution on Phtalocyanine Based Compounds for Photovoltaic Application. International Journal of Chemistry and Materials Research, 2015. **3**: p. 65-78.*
*(b) Segawa, Y., H. Ito, and K. Itami, Structurally uniform and atomically precise carbon nanostructures. Nature Reviews Materials, 2016. **1**: p. 15002.*

Table 1. Classification and main biomedical applications of nanoparticles [1].

Nanoparticle	Chemical composition	Principle of application	References
CNTs	Pure carbon	Diagnostic and sensing element to detect and monitor several diseases, especially diabetes but also bacterial infection.	[53]
		Selective reactivity with certain biomolecules.	[39]
Fullerenes	Pure carbon	Selective reactivity for antiviral activity.	[36, 37]
Metal oxides	ZnO	Excellent biocompatibility. Anticancer and antibacterial agent.	[54]
	Silica	Drugs and gene delivery.	[55]
	TiO_2	Photodynamic therapy and delivery of different anticancer drugs.	[56]
	TiO_2	Positive effects on strength and growth of plants.	[57]

	CeO	Enzyme mimetic and reactive oxygen species (ROS) scavenging activities.	[58]
	CuO	Antimicrobial agents.	[59]
	Al_2O_3	Oral drug delivery, biosensing, cancer therapy and anticancer properties.	[60]
	MnO_2, ZrO_2	Antibacterial and anti-inflammatory features.	[61]
	Iron oxides	Antimicrobial activity, magnetic hyperthermia (superparamagnetic properties).	[62, 63]
		Medical diagnosis: Sensors for microbial detection.	[32]
Quantum dots (QDs)	CdSe	Medical diagnosis: Luminescence properties for labelling bacteria.	[52]
	CdS	Biomedical imaging: Biomarkers.	[24, 42-44]
	CdSe/ZnS	Biomedical imaging: Bioactive fluorescence; immunoassay applications.	[25, 52]
Metallic NPs	Ag	Antimicrobial properties.	[45-48]
		Localized surface plasmon resonance.	[45-48]
		Antibacterial activity.	[64]
	Au	Surface plasmon resonance.	[30, 31, 65]
	Au	Conjugation with biomolecules.	[66, 67]
Polymers	Alginate/chitosan	Slow drug delivery.	[51]
		Encapsulated, adsorbed or dispersed bioactive compounds maintaining their structure, activity and releasing over a longer time.	[68]

*(Reference: López-Serrano, A., et al., Nanoparticles: a global vision. Characterization, separation, and quantification methods. Potential environmental and health impact. Analytical Methods, 2014. **6**(1): p. 38-56.)*

1.4. Immunogenicity and biocompatibility of nanomaterials

1.4.1. Biodistribution and stability of NPs in the biological environment

The biodistribution of the inorganic NPs, within the *in vivo* biological environment, has been intensively investigated, including quantum dots and superparamagnetic NPs. The bare inorganic core of NPs will not be stable within the biological conditions; therefore, it always occurs within organic coating, either chemically designed during developing the NPs or obtained by the adsorbed surrounding proteins [69, 70] (**Figure 4**). Otherwise, without the organic coating, the plain NPs tend to aggregate [71].

Theoretically, the ideal NP is defined as hybrid entity of three parts: inorganic core, surface coating and external adsorbed compounds from the surrounding biological

environment. However, in this study we did not investigate the outer layers coating of the inorganic core.

The identity of the NP is described according to the nature of its core, which defines its physical features, *e.g.*, superparamagnetic or fluorescent [72]. Therefore, the core is responsible for many vital approaches, such as exhibiting the contrast within imaging and detection techniques or rising heat by excitement within hyperthermia procedures. However, maintaining the physical properties of the core within the biological environment is essential, especially within theranostic approaches. Therefore, biotransformation occurring to NPs, *e.g.*, degradation or aggregation, may imperil those physical properties according to the surrounding environment.

Previous studies have shown that semiconductor Si is an ideal model to be employed as core biomaterial owing to its promising features, since it can occur in several biocompatible designs, in addition to its competence to bind to living tissues. Furthermore it was demonstrated to be fully biodegradable [73].

The surface coating plays also a critical role to define the physicochemical properties of the NPs, known as "synthetic identity" [74]. The surface coating can be of different kinds of molecules, *e.g.*, lipolic acids, peptides or silica shells [75, 76]. The subsequent physicochemical properties of NP, *e.g.*, hydrophobicity and surface charge determine its colloidal stability. Therefore, proper NPs surface coatings should tackle agglomerations of NPs and enhance dispersion in the surrounding environments. And achieving this depends on many factors within biological environments, *e.g.*, which molecules adsorb to the surface, cellular uptake and even cell viability.

Within the biological environments, some degree of *in-situ* biotransformation has to occur for most of NPs, *i.e.*, adsorption of the surrounding molecules on the surface of NPs forming what is known as "biomolecule corona", of which protein corona (PC) has been widely investigated, which is now well recognized, but still not well understood [69, 77-82].

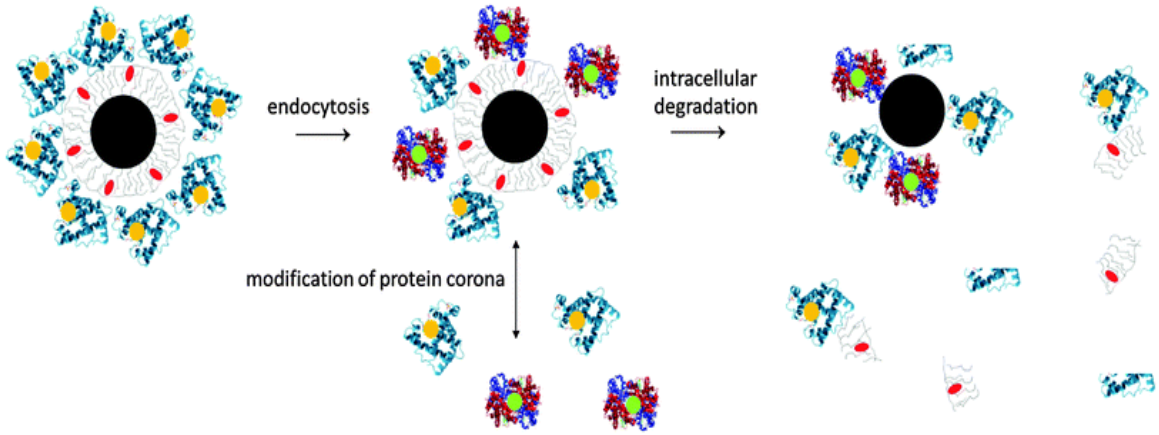

Figure 4: Illustration of an inorganic NP within *in vivo* biological environment composed of inorganic core (black circle), enveloped by organic coating (grey color) which assists the colloidal stability and an outer layer of adsorbed proteins (blue color), within the *in vivo* circumstances, NPs tend to change their physicochemical features, including dynamic altering of the protein corona, according to the changes in the biological surrounding conditions or the mechanisms of cellular degradation that may even degrade the NP into tinier individual fragments. Moreover, some inorganic cores might decompose, and thus, alter the physical and morphology. Likewise, the organic coating can be partially detached while the adsorbed proteins are being degraded.

(Reference: Feliu, N., et al., In vivo degeneration and the fate of inorganic nanoparticles. Chemical Society Reviews, 2016. 45(9): p. 2440-2457.)

1.4.2. **Cellular interaction and bio-fate of NPs**

It has been shown in several cell based studies how cells react with NPs during administration, whereas most of mammalian cells have shown different capacities to incorporate NPs, owing to different nonspecific uptake mechanisms [83]. Nevertheless, under *in vivo* circumstances, some mammalian cells are capable of significantly degrading those NPs. The interactions occurring *in vivo* between close tissues, lead certain cells to break down any foreign particles, *e.g.*, NPs. For instance, the macrophages within the mononuclear phagocyte system (MPS) are known to possess high potency to clear and process large NPs from the blood stream, whereas, most of the other cells are lacking the sufficient capacity to incorporate and process the NPs. However, it is worth mentioning, that within *in vivo* conditions, the clearance of NPs vastly alters, according to the status of the immune system [84]. Subsequently, degradation of NPs under *in vivo* conditions, is highly dependent on many factors, such as the physicochemical properties

of the NPs and the type of the cell exposed to the NPs, which can also determine the biodistribution and intracellular transfer of the NPs.

NPs based biomedicines are commonly introduced as bolus injection intravenously. Next, the blood stream carries the NPs to the right chamber of the heart, then to the lung, back to the left heart chamber then to the arterial system distributing the NPs to different organs. During this transporting process, a large blood portion arrives to the liver and spleen, which possess high potency to filtrate the blood and eliminate xenobiotic particles, *e.g.*, NPs. Several quantifications experiments have estimated distributions of labelled NPs and they found that huge portion of protein coated NPs were incorporated and trapped by these organs [85, 86]. Endothelial cells are as well a secondary adequate receiver of those NPs *in vivo*. Since, these endothelial cells are lining the blood vessels around the body they got in direct contact with the administrated NPs [87]. **Figure 5** [71] shows an overview of the whole uptake process, collected from different articles [85, 88-90].

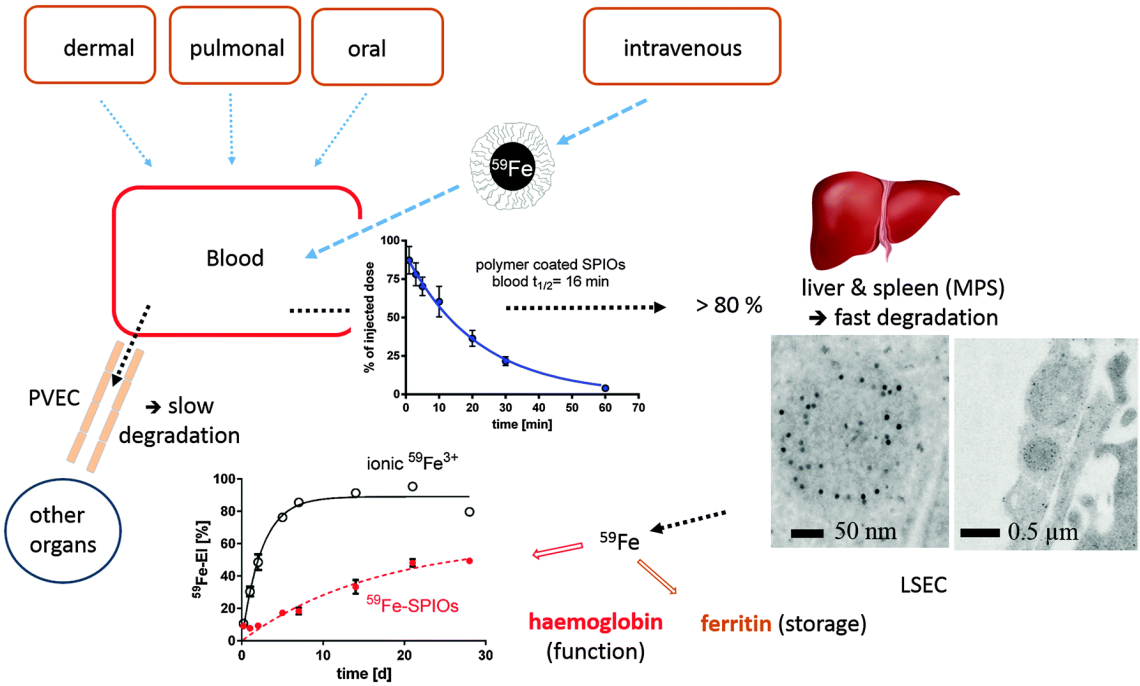

Figure 5: Fe-labeled FeO_x NPs were injected in mice intravenously and their distribution and degradation were monitored. These NPs exhibited a 25 nm diameter, carrying surface negative charge and composed of monodisperse iron oxide core with 11 nm diameter, coated with amphiphilic polymer, poly(maleic anhydride-*alt*-1-octadecene). Liver cells, *i.e.*, Kupffer cells and liver sinusoidal endothelial cells (LSECs), were detected incorporating large portion of the NPs within minutes. Furthermore, the degradation of the FeO_x core was estimated by measuring the amount of Fe presented in the hemoglobin of the lately produced red blood corpuscles. Nevertheless, peripheral vascular endothelial cells (PVECs), are another reservoir to receive FeO_x NPs.
However, the outcome of monitoring the degradation of FeO_x NPs, exhibited a notably degradation efficacy difference among the different sorts of cells, proposing that the NPs undegraded residues are possibly remaining in the cells causing a cell specific long-term toxicity.

MPS = mononuclear phagocyte system (mainly liver and spleen).

(Reference: Feliu, N., et al., In vivo degeneration and the fate of inorganic nanoparticles. Chemical Society Reviews, 2016. 45(9): p. 2440-2457.)

1.4.3. **Immune response to NPs**

Nanotechnology based drug delivery systems may be designed to recognize a biomarker in certain tissues of a specific patient. However, these systems are susceptible to be recognized and targeted by the immune system as an outsider body. Even though, there are several studies have been conducted to understand these immune responses, it is still challenging to have a clear interpretation, because the immune responses vary intensively between different lab animals and humans, which makes the immune response in human bodies difficult to predict [91].

There is a study conducted by Bremer-Hoffmann and Halamoda-Kenzaoui *et al.* [91] from the European Commission Joint Research Centre (JRC), Ispra (VA), Italy, that reviews different scientific literature and concludes the most recurrent *in vivo* immune response induced by different nanomaterials are inorganic NPs, lipid-based and polymer-based NPs (**Figure 6A**) [91], of which, inorganic NPs were found to be responsible for ~68% of the explained immune reactions. The results showed that approximately 50% of the examined NPs provoked reactions that triggered immune response. The most immediate immune response occurs upon intravenously administration. Prompting the immune reactions can be favorable to the host animal because it can assist recognizing and removal of any harmful invasive materials. Some NPs based trails have shown noticeable positive medical effects, for instance, Au nanorods have exhibited suppressing effect on respiratory syncytial virus and also stimulating an antiviral reactions in mice models [92].

Human immune system adopts two main defense mechanisms: innate immune and adaptive immune mechanisms. Under microbial attack, the innate system provokes nonspecific reactions to tackle the microbial invasion, however, the adaptive system joins later with more specific reactions, including stimulating the lymphocytes and synthesizing consequent antibodies. It is worth mentioning, NPs were exhibited immune reactions to both innate and adaptive immune systems, either provoking or quelling (**Figure 6B**) [91]. Moreover, the immune responses are highly dependent on structure of the NPs protein corona layer.

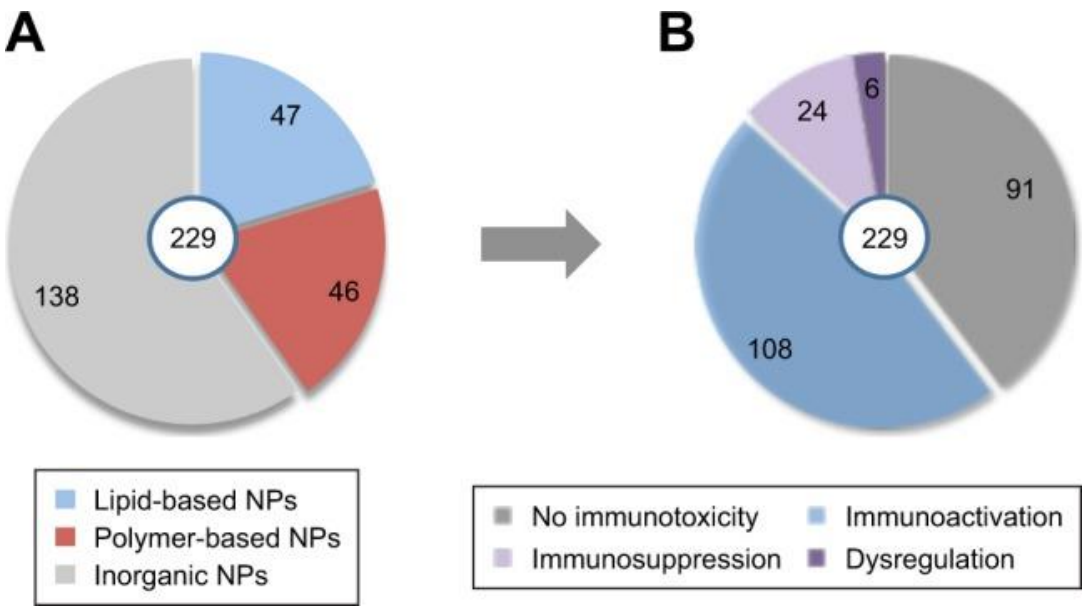

Figure 6: (A) The outcome of the reviewed *in vivo* studies showing the main NPs to provoke immune responses, whereas inorganic NPs was the major group with an approximate percentage of 68%. **(B)** The main various immune responses provoked by NPs, showing immunoactivation to be the major immune response.

(Reference: Halamoda-Kenzaoui, B. and S. Bremer-Hoffmann, Main trends of immune effects triggered by nanomedicines in preclinical studies. International journal of nanomedicine, 2018. 13: p. 5419-5431.)

In **Figure 7** [91], the most reoccurring NPs-based immune responses were described, in corresponding to NPs groups. In conclusion, 61% of the articles describing lipid-based NPs immune effects, mentioned that the main effects are activating the complement system, complement activation-related pseudoallergy (CARPA), in addition to activating the adaptive immune system. On the other hand, ~65% of evaluated polymer-based NPs were identified as immune friendly and did not exhibit any potential immunotoxicity. However, these polymer-based NPs were commonly provoking an antigenicity response convoyed by releasing of specific antibodies, in signaling cascades lead to accelerated blood clearance (ABC) of those nano compounds. Lastly, 70% of the examined inorganic NPs showed a negative effect on the immune systems, especially, an escalated threat of inflammation accompanied by innate or adaptive immune response.

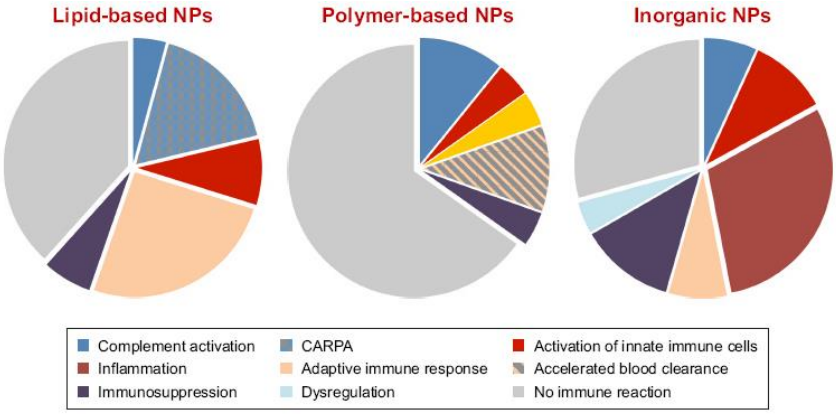

Figure 7: The figurers illustrate the most common *in vivo* NP-induced immune responses, categorized based on the nature of the NPs. Nevertheless, the type of immune responses depended on the nature of the NPs. Thus, polymer-based NPs exhibited the most immune friendly effect, meanwhile inorganic NPs were the least friendly with several immune responses, mainly inflammation. Lipid-based NPs provoked several immune responses, including complement activation-related pseudoallergy (CAPRA) and adaptive immune response.

(Reference: Halamoda-Kenzaoui, B. and S. Bremer-Hoffmann, Main trends of immune effects triggered by nanomedicines in preclinical studies. International journal of nanomedicine, 2018. 13: p. 5419-5431.)

Among 108 literatures within this study (Hoffmann and Kenzaoui) reporting immune activation reactions by NPs, 43 described the inflammatory procedures to comprise proinflammatory cytokines production and inflammatory histological changes (**Figure 8**) [91]. Nevertheless, the NPs-induced inflammation mechanisms were concluded to occur in main forms, including oxidative stress initiation, toll-like receptors recognition, which is responsible for pathogen identification, and activating corresponding inflammatory pathways, *e.g.*, cellular nuclear factor-κB. Mainly, the inflammatory responses were attributed to inorganic NPs, primarily silica NPs [93], carbon/metal based NPs , Au NPs [94, 95] and graphene oxide-based nanomaterials [96, 97].

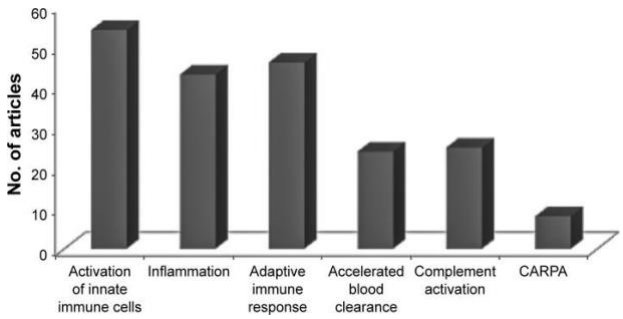

Figure 8: Based on the reviewed literatures, the most reported NPs-based immune response happening in high reoccurrence.

CARPA = complement activation related pseudoallergy.

(Reference: Halamoda-Kenzaoui, B. and S. Bremer-Hoffmann, Main trends of immune effects triggered by nanomedicines in preclinical studies. International journal of nanomedicine, 2018. 13: p. 5419-5431.

1.4.4. **Role of inflammatory response in liver diseases and oxidative stress**

Inflammation is considered as potential sign indicating existence of harm conditions or organisms, and it can even refer to cancer development when paired with tumorigenesis [98]. Pathogenic microorganisms are detected through a key signaling platforms called "inflammasomes", which are also responsible for activating the corresponding inflammatory response.

Hepatic tissue damage is attributed mainly to hepatic inflammation, which is also considered as common provoker of liver diseases [98]. Under hepatic inflammation conditions, liver experiences progression from nonalcoholic fatty liver disease (NAFLD), which is defined as an accumulation of fats, approximately >5%, in liver cells for a reason else than excessive alcohol consumption [99], to fibrogenesis and ultimately hepatocellular carcinoma (HCC).

Oxidative stress and lipid peroxidation are strong consequences of the liver inflammation and damaged liver, which frequently trigger characteristic histological lesions of NAFLD [100, 101]. Under liver inflammatory circumstances, the inflammatory cells and the hepatocytes discharge cytokines, *e.g.*, tumor necrosis factor alpha (TNF-α) and reactive ROS, which can prompt peroxidation of plasma and mitochondrial membranes, leading to cellular death owing to necrosis and apoptosis [100, 101].

As mentioned earlier, liver represents an ultimate harbor for the intravenous administrated NPs, where NPs are incorporated and trapped though blood filtration process. Consequently, it is worth studying the inflammatory response and effect of those NPs on the liver.

Therefore, in this work we aimed to investigate the immunomodulatory and biological effects of a widely used inorganic NPs, such as porous silicon (PSi) NPs, on liver functions.

1.5. Nanomedicine today and future aspects

There is a very rapidly growing number of applications within the nanomedicine field, including drug delivery, thermal assays, *e.g.*, hyperthermia, and imaging. Moreover, in medical diagnostics, nanotechnology is contributing a huge advance, as these require an accurate identification of the targets, *e.g.*, tissues, cells and receptors, that correspond to certain medical disorder, thus designing the perfect matching NPs, which accomplish the required reaction with the least side effect [20].

Nanomedicine represents promising tools to transform the increasing medical discoveries into practical treatment for patients, including these NPs that mimic the biological system, *e.g.*, those that are efficient in early diagnosis and cancer targeted drug delivery therapies.

Likewise, there are verities of fascinating rising effective technologies for targeting diverse cell types within the body optimizing the delivery of cargo, *e.g.*, drugs, genetic materials, diagnostic elements or any else medical therapies. Thus, currently, drug delivery and diagnostic assays are the leading projects within the nanomedicine field.

1.6. Porous silicon nanoparticles (PSi NPs)

Electrochemical etched PSi has attracted attention for various biological applications due to its exceptional features, *e.g.*, biocompatibility [102], biodegradability [103] and tunable porous nanostructure [104], which is highly advantageous for drug delivery approaches.

In 1956, porous silicon (PSi) was discovered by Uhlir accidently, when he was conducting some electropolishing studies on Si wafers with hydrofluoric acid. During his experiments he discovered that under certain circumstances of suitable current and solution constitution, the Si did not dissolve homogeneously, and fine holes were formed instead. Subsequently, Si wafers were utilized to produce PSi, by electrochemical dissolution of the Si wafers in aqueous or ethanoic hydrofluoric acid solutions [105]. Since then there was no much attention drawn towards PSi, until 1995 when PSi was verified by Canham to be biocompatible and biodegradable [103].

After that, PSi was under intensive investigated in biomedical applications, owing to its unique features: (1) high porosity / large pore volume (up to 80% / ≈ 0.5–2.0 cm^3/g) which is perfect for high loading degree; (2) adjustable surface chemistry and enormous surface area (up to 580 m^2/g), this surface can be functionalized for several biological functions like controlling drug release [104, 106]; (3) modifiable pore size (≈ 5 – 150 nm) to load various molecules, including macro- ,small- and NPs [107, 108].

Moreover, PSi is promising for drug delivery and other biomedical applications, *e.g.*, bioimaging, tissue engineering and immunotherapy applications [109]. Another advantage of utilizing PSi is its great biocompatibility since it can be completely degraded to nontoxic orthosilicic acid [$Si(OH)_4$], which is naturally occurs in the human body [103, 110, 111].

1.6.1. Fabrication of PSi

Commonly, PSi is synthesized by electrochemical anodization of monocrystalline Si wafers in a hydrofluoric acid electrolyte solution. Furthermore, the porosity and pore size can be modified through manipulating the manufacturing parameters, thus the biodegradability of a PSi structure can controlled accordingly with its the pore size and porosity [109]. Therefore, PSi has been found of great advantage in drug delivery applications, whereas, the pore sizes can be adjusted according to the properties of the loaded drug and the release mechanism [104].

There are different forms of PSi being utilized in biomedicine, according to the purpose. However, the spherical shaped (quasi) PSi micro- and nanoparticles are the most abundant form within drug delivery systems, owing to their broad selections and being easy to produce. In the following section, the fabrication process of spherical shaped (quasi) PSi is described.

1.6.1.1. Fabrication of spherical shaped (quasi) PSi

The technology of engineering PSi micro- and nanoparticles has developed remarkably recently, and those produced PSi particles have attracted much attention. PSi is described

as nanostructured material manufactured frequently through etching single-crystal Si wafers [109]. As mentioned earlier, PSi is commonly produced in top-down approach through electrochemical anodization of monocrystalline Si wafers in a hydrofluoric acid electrolyte solution. After the anodization process, a PSi film is separated from the Si wafers as whole thin chips (**Figure 9a**) [109]. Afterwards, comes the comminution step, and it can be accomplished through different approaches, *e.g.*, ultrasonication [112], high pressure micro-fluidization [113] or milling [114]. Ultimately, the outcome is PSi spherical shaped particles (quasi).

During the PSi NPs fabrication procedure, there are main principles to consider: (**1**) ultrasonication is mainly employed to obtain PSi NPs smaller than 300 nm [112] (**Figure 9b**) [109]. Moreover, the size can be highly decreased till 50 nm approximately, by involving high power ultrasonication (**Figure 9d**) [109]; (**2**) high shear microfluidization is another approach for synthesis PSi particles, however it is faster than ultrasonication, and can produce high yield of PSi NPs with narrow size distribution [113, 115]. PSi NPs are produced by both approaches; microfluidization and ultrasonication (**Figure 9c**) [109]; and (**3**) PSi NPs can be created through an alternative bottom-up pathway, whereas PSi NPs are built from silicon tetrachloride.

Within this approach, a byproduct salt is formed within the produced NPs and it assist to form the pores through acting like a template. Afterwards, this byproduct salt is washed away through simple water rinsing step, leading to porous structured nanoparticles [106] (**Figure 9e**) [109]. This bottom-up strategy has the advantage of avoiding the harsh etchants like hydrofluoric acid. Another advantage of this bottom-up approach, is the possibility of adjusting the average size, pore diameters and specific surface area of the produced PSi NPs, as described by Fang Dai *et al.* [116], whereas three temperatures were involved within PSi NPs fabrication process: 600, 700 and 820 °C. All of these temperatures exhibited PSi NPs with similar mesoporous structures. However, under the high resolution transmission electron microscope (HR-TEM), the crystallite sizes of the PSi NPs were different: PSi-600 = 3-5 nm, PSi-700 = 7-10 nm and PSi-820 = 10-20 nm. (**Figure 9f-h**) [109]. Furthermore, the outcome PSi NPs from this approach presented higher surface area (≈ 580 m_2/g) than those PSi NPs produced by electrochemical etching.

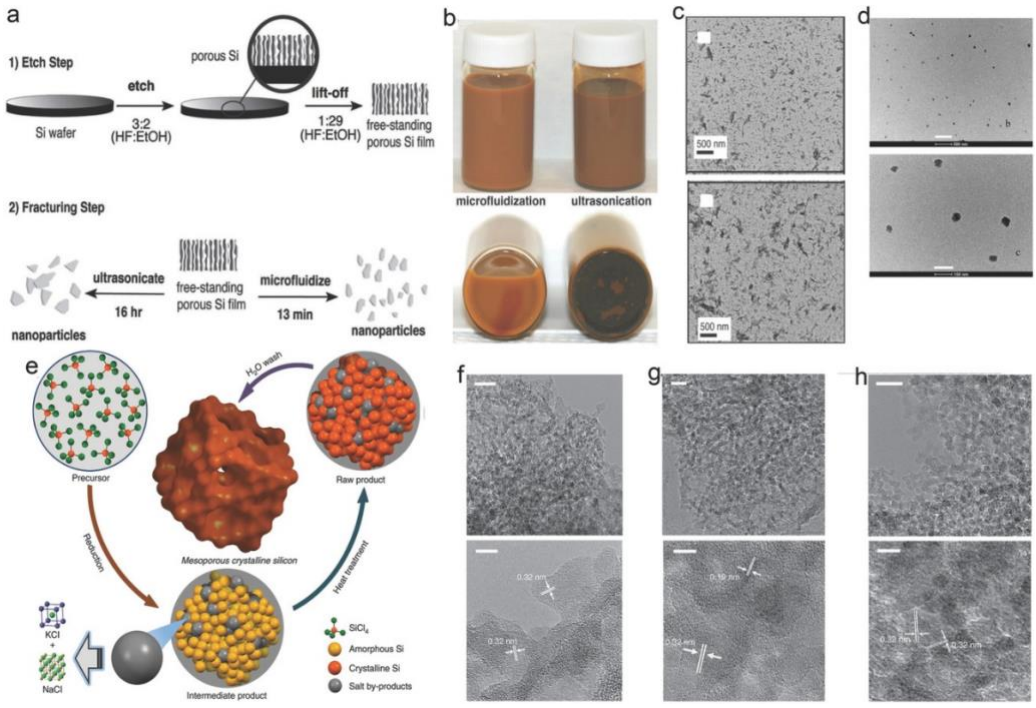

Figure 9: Fabricating PSi spherical (quasi) particles. **a)** The first step, etching, followed by two alternative techniques; ultrasonication and shearing thought micro-fluidization. **b)** Outcome PSi NPs contained in vials, micro-fluidization product (left) and ultrasonication product (right). **c)** TEM Images of both techniques' PSi NPs product, micro-fluidization (top) and ultrasonication (down). **d)** TEM images of PSi NPs fabricated by high power ultrasonication, in two different scales: 500 nm scale bar (upper), and 100 nm scale bar (down). **e)** Illustrating diagram of the bottom-up fabrication process of PSi particles. **f-h)** TEM images of PSi particles fabricated under different temperatures; f = 600 °C, g = 700 °C, h = 820 °C. The upper images are produced by TEM with scale bar 20 nm, while the lower Images are produced by HR-TEM with scale bar 5 nm.

*(Reference: Li, W., et al., Tailoring Porous Silicon for Biomedical Applications: From Drug Delivery to Cancer Immunotherapy. Advanced Materials, 2018. **30**(24): p. 1703740.)*

1.6.2. **PSi with different Surface Chemistry**

As mentioned before, bottom-up approaches for fabricating PSi NPs are preferred due to speed of the process and avoiding harsh etchants, nevertheless, electrochemical etching strategy is still the dominant method to produce the PSi involved in the biomedical applications, *e.g.*, drug delivery systems [117, 118]. PSi recently fabricated by electrochemical etching possess some drawbacks which might conflict with their functioning upon involving in biomedical application strategies. For instance, the freshly fabricated PSi are extremely reactive owing to their hydride terminated surface [119], which makes the surface not stable chemically because the ongoing slow oxidation due to exposing to atmosphere air. Subsequently, this oxidation may trigger structure and optoelectronic alteration of PSi, in addition to possibility to react with several biological

materials and the loaded cargo [120]. Consequently, it is highly recommended to chemically modify PSi surface upon incorporating in biomedical applications, especially, drug delivery systems.

Here, three different surface modifications are presented: thermally oxidized PSi, thermally carbonized PSi and undecylenic acid-modified thermally hydrocarbonized PSi. Direct thermal oxidation is commonly applied oxidation method for stabilizing the surface of PSi. In this direct oxidation process, the temperature is raised to 300-400 °C, whereas the oxygen bonds are built between surface Si atoms. Then, the temperature is escalated again to more than 600 °C, so the oxidation is boosted and all SiH_x species are eliminated [121] (**Figure 10**) [109]. Nevertheless, there are other oxidation approaches, *e.g.*, chemical oxidation [122], aqueous oxidation [123], photooxidation [124] and anodic oxidation [125]. Eliminating Si_xSiH_y bonds and establishing O_ySi-OH and Si-O-Si species are common features among those oxidation strategies. Furthermore, it was noticed from experiments that these oxidation modifications alter also the properties of PSi surface from hydrophobic to hydrophilic [126], which may work in favor of several drug delivery strategies within physiological environments.

Another approach for stabilizing PSi surface is thermal carbonization, which is categorized to two approaches according to the temperature of the process: (**1**) Thermally hydrocarbonized PSi (THCPSi), accomplished at lower temperature 400-600 °C; and (**2**) Thermally carbonized (TCPSi), accomplished at higher temperature >600 °C [104, 127, 128] (**Figure 10**) [109]. In addition to stabilizing the PSi surface chemistry through this process, due to the comprehensive coverage of the innate silicon hydride surface, this process does not affect the functioning surface area of PSi [129]. Furthermore, TCPSi are characterized by more hydrophilic surface chemistry, which is more stable than THCPSi [130].

Last, a PSi stabilizing and functionalizing method is used through adding some chemically reactive groups carboxylic acids (-COOH) and amines ($-NH_2$), through some specific reactions, *e.g.*, hydrosilylation and silanization [131] (**Figure 10**) [109]. From such reaction, undecylenic acid functionalized THCPSi (UnTHCPSi) are obtained. This approaches are characterized by mild procedures since the some surface alterations can be accomplished in room temperature [132], in addition to wide alternatives of adding

variant functioning reactive groups, *e.g.*, PSi terminated with carboxylic acid and alkenes [106].

Overall, these surface stabilizing approaches are conducted according to the purpose of use in the medical application and according to the chemical properties of the loaded cargo [109].

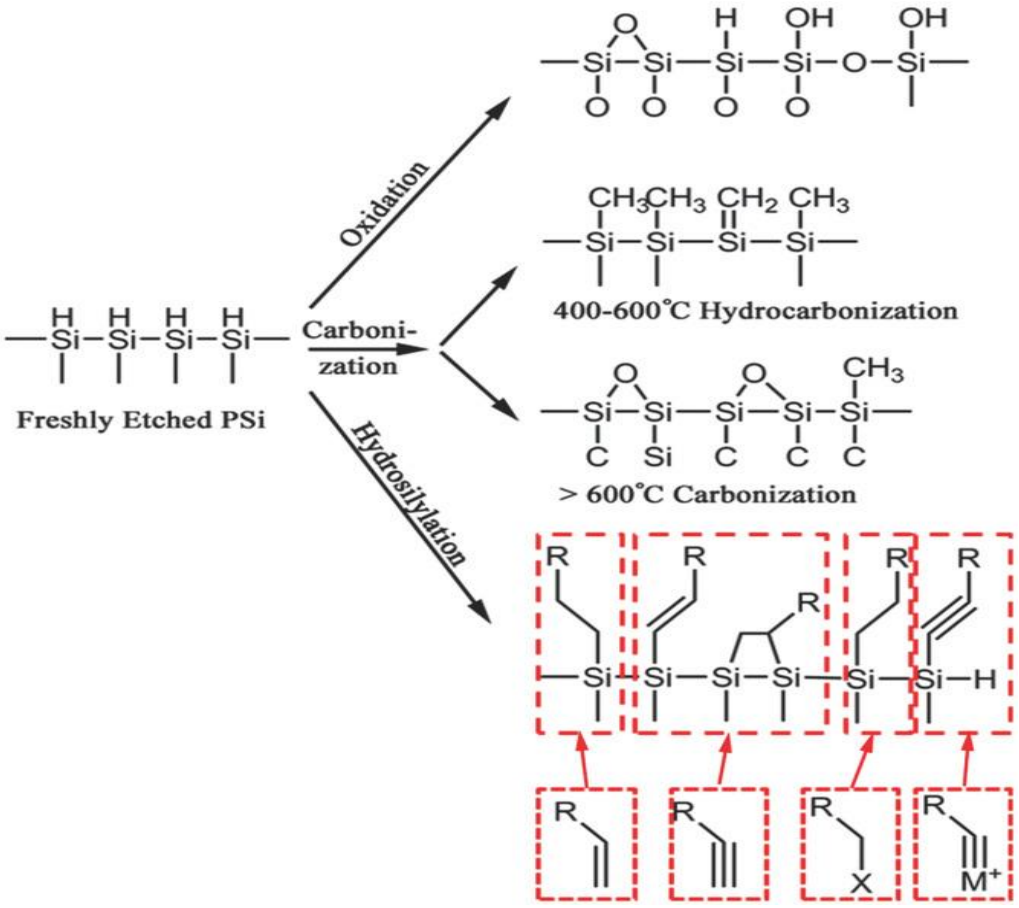

Figure 10: Different surface modifications approaches of newly etched PSi, in order to produce variant PSi material with different surface chemistry, *e.g.*, through oxidation, thermally oxidized TOPSi with hydrophilic surface can be produced. Thermally carbonized TC and thermally hydrocarbonized THCPSi can be produced through carbonization approach, which involves thermal decomposition of acetylene in temperature range 400-900 °C, thus TC and THC PSi are harvested separately in a higher and a lower temperature, respectively. Lastly, stabilizing and functioning PSi through hydrosilylation method using Lewis acids in presence of unsaturated compound, *e.g.*, alkynes. This approach is beneficial to produce undecylenic-acid-modified thermally hydrocarbonized PSi, UnTHCPSi, with possibility to assemble different functional groups on the surface, e.g., alkenes and amine groups.

(Reference: Li, W., et al., Tailoring Porous Silicon for Biomedical Applications: From Drug Delivery to Cancer Immunotherapy. Advanced Materials, 2018. ***30****(24): p. 1703740.)*

1.6.3. **Reductive nature of PSi NPs**

As demonstrated earlier, the recently etched PSi possessing Si hydride surfaces exhibit high reductive properties, which can boost reaction with several biological material within the surrounding environment. During the investigation, it was found that under certain circumstances, PSi hydride surface is able to produce single oxygen ($^1O_2$) molecules that may trigger cellular toxicity. Thus, surface modifications can reduce and eliminate that toxicity effect, meaning better biocompatibility [133, 134].

Another advantage of surface modification is controlling the biodegradation of PSi, which is critical element to be evaluated before incorporating in clinical applications. Freshly etched PSi endures quick disintegration due to surface high reactivity, therefore, surface modifications, *e.g.*, oxidation and carbonization can create a protection and restrain this degeneration process [135, 136].

There are several factors that can affect the degradation kinetics of PSi including temperature, pH, salinity in addition to redox environment [137]. In some studies, *in vitro* PSi degradation under influence of pH, human serum and ROS was investigated [138]. This study presented ROS is the most influencing factor on the PSi erosion process, since it can expedite the degradation significantly. Within PBS buffers with different pH (7.4 and 6.5), PSi degradation exhibited unaffected manner, whereas PSi ML_{50} (which is the time required for half of PSi mass to degrade) [109] was approximated 7 h at either pH degrees. Adding human serum reduced ML_{50} to 6 h. On the hand, adding 2×10^{-3} M of 3-morpholinosydnonimine N-ethylcarbamide (SIN-1), which is usually employed to physiologically provoke production of peroxynitrite, an extremely ROS occurred in human carcinogenesis, which could dramatically reduce the PSi ML_{50} to 3 h.

Furthermore, upon *in vivo* administration, it was discovered that PSi experience increased degradation within diseased conditions, due to presence of escalated levels of ROS, because of the upregulation response in the inflamed region, thus Si scaffolds are oxidized by ROS compounds into Si-dioxide, followed by hydrolysis of Si-O bond eventually leading to soluble orthosilicic acid species [110, 139], *i.e.*, enhanced degradation process.

After previously mentioned surface stabilizing modifications, carbonization and oxidation) the PSi surface is constituted of either silicon carbide SiC or O_xSiH_y terminates, which are chemically stable, and ROS induced degeneration process correlate the degradation to the decomposition of the Si layer and back-bond oxidation of Si [138].

Nevertheless, the ROS degradation effects on surface modified PSi are still not well understood and lack of investigation.

1.6.4. **Immunogenicity and biocompatibility of PSi NPs**

We mentioned earlier that biomedical studies have demonstrated PSi to be competent apparatus for transferring therapeutics, nevertheless, nowadays there is more attention towards evaluating the immunogenic properties of these PSi materials [140]. Ainslie *et al.* [141] examined the immunogenic properties of several Si platforms (nanoporous, microstructured, nanochanneled and flat), and found that those platforms were able to provoke secretion of some proinflammatory cytokines by peripheral blood mononuclear cells (PBMCs). Likewise, other different studies have presented that PSi micro- and nano-particles with different surface characteristics, were also able to induce distinctive immune reactions [142-144].

The immunogenic properties of PSi NPs with different surface chemistry was investigated in another study by Shahbazi *et al.* [144], whereas other engineered PSi NPs were included in the study: poly(methyl vinyl ether-alt-maleic acid) conjugated APSTCPSi (APM), polyethyleneimine conjugated UnTHCPSi (UnP) and (3-aminopropyl)triethoxysilane functionalized THCPSi (APSTCPSi). Human monocyte-derived dendritic cells (DCs) were incubated with those PSi nanoparticles, in cytocompatible concentration 25 µg/mL. The result showed two PSi surface modifications (THCPSi and TOPSi) to cause high immunostimulating effect. Immunogenicity of THCPSi was explained according to their hydrophobicity [145, 146]. Meanwhile, the immunogenicity of TOPSi was attributed to immunogenic effect of the orthosilicic acid produced upon the degradation process of TOPSi within the physiological environment [144, 147] .

In addition, the other PSi NPs (thermally carbonized-TCPSi, and UnTHCPSi) did not exhibit significant increase of the correlated co-stimulatory signals (CD80,83,86 and human leukocyte antigen-D related (HLA-DR)), **Figures 11a and 11b** [144]. Furthermore, THCPSi and TOPSi provoked TH1-biased immune response, recognized by the secretion of interleukin-12 (IL-12) and IFN-γ, in addition to the priming $CD8_+$ T-cells, remarkably when incubated with TOPSi (**Figures 11c and 11d**) [144].

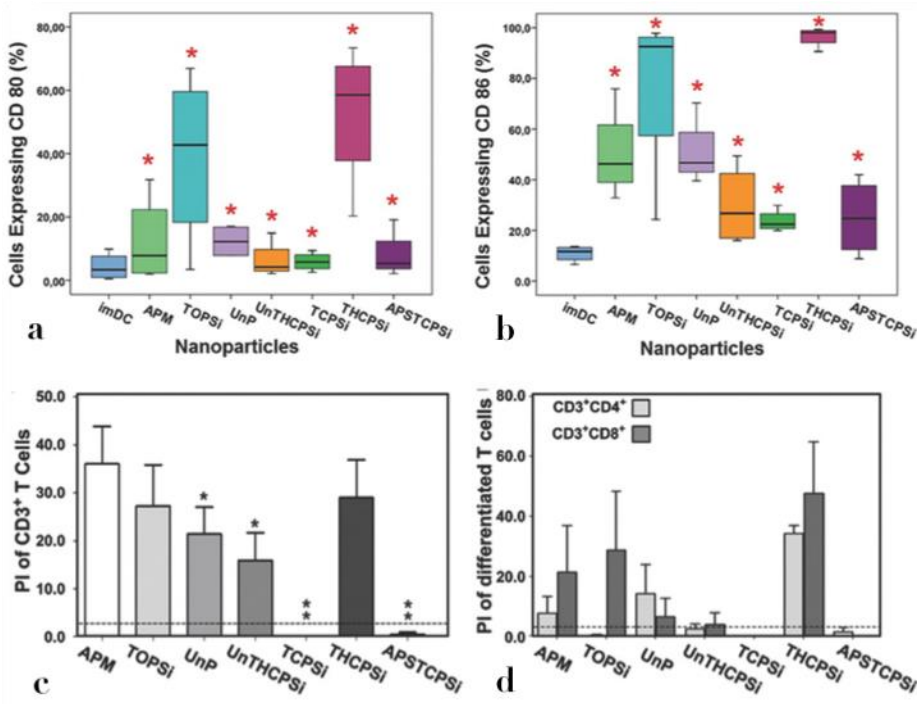

Figure 11. Different co-stimulatory signals expressed by human monocyte derived DCs representing the immune response towards PSi NPs with different surface chemistry: **a-b)** Percentage of expressed CD80 and CD86 after incubation with 25 µg/mL PSi NPs for 48 h. Cells were stained by specific antibodies against each marker and examined by flow cytometry. The outcome readings for each PSi NPs were compared with imDC (untreated human monocyte-derived dendritic cells (MDDCs)), which are featured by their negligible expression of DC maturation markers) as control. **C-d)** Illustration of lymphocyte response upon 6 days incubation with 25 µg/mL PSi NPs, showing the effect of different PSi NPs on inducing proliferation of $CD3_+$, $CD4_+$and $CD8_+$ T cells. Most of PSi presented an immune stimulating effect, however, TCPSi solely did not exhibited any induction of neither $CD3_+$, $CD4_+$ nor $CD8_+$ T cells. TOPSi were able to induce $CD8_+$ and $CD3_+$ but not $CD4_+$. UnTHCPSi exhibited only induction of $CD3_+$.

*(Reference for this model: Shahbazi, M.-A., et al., Surface chemistry dependent immunostimulative potential of porous silicon nanoplatforms. Biomaterials, 2014. **35**(33): p. 9224-9235..)*

1.6.5. Biomedical applications of PSi NPs

1.6.5.1. Drug delivery

PSi possesses various features that make it an attractive apparatus for drug delivery approaches: the electrochemical synthesis permits building verities of controllable tailored pore sizes; abundant chemistries to modify PSi surfaces that can be employed to control the amount, type and release rate of the loaded drug; and importantly, the optical specifications of photonic porous Si structures which facilitates *in vivo* self-reporting and monitoring. However, there are current key challenges of drug delivery systems, *e.g.*, poor solubility of drug molecules, fast clearance of drug from the body or inadequate drug release. Thus, PSi NPs are proposed as potential candidate to overcome this issue, *i.e.*, to increase the bioavailability of the drug molecules within certain area and over defined time frame. Upon containing the drug cargo inside the pores of PSi, the constricted space of PSi NPs prevent the drug to return back into its crystalline form (lower solubility) and remains in amorphous form (higher solubility), meaning more control on the drug releasing/dissolution rate [148]. For instance, saliphenylhalamide (an antiviral drug with low water solubility) was loaded inside THCPSi NPs to minimize the crystalline form of this drug, and after applying this construction on influenza A virus infection, the results were very promising. Upon releasing this antiviral drug from PSi NPs, an efficient inhibition of influenza A infections was demonstrated in human retinal pigments epithelium and Madin-Darby canine kidney cells [149].

PSi NPs are promising candidates for cancer drug delivery as well, especially because most of anti-cancer drugs are very poor water soluble. As an example of this, when cisplatin (anti-cancer drug) was loaded in 1,12-undecylenic acid modified PSi microparticles, a higher toxicity was detected than the free form of cisplatin in human ovarian cancer cells, due to the enhanced solubility [150].

Various protein molecules can also be delivered through PSi NPs. For instance, agarose hydrogel matrix was used to adjust the surface of PSi particles for sustain administration of bovine serum albumin over long period, meanwhile maintaining the molecular characteristics and stability of the protein [151]. Furthermore, PSi NPs have exhibited

great ability to preserve the bioactive form of the protein drugs providing protection of the enzymatic degradation and enhance the bioavailability in targeted site [152].

Therapies based on delivery of oligonucleotides have always confronted low intracellular delivery due to the negative charge on those oligonucleotides. Thus, PSi NPs have been recently proposed as efficient carrier for those therapeutics to improve cellular delivery and protect them against enzymatic degradation [153-155].

Small interfering RNA (siRNA) molecules were loaded in PSi NPs by Wan *et al.* [156], whereas they were able to load about 7.7 µg of siRNA per mg of PSi NPs within time range of 30 min. Upon applying this formulation, 33% of cell apoptosis was induced through downregulating the corresponding mRNA and following protein expressions.

All of the aforementioned applications propose PSi NPs as a potential future material for many drug therapies and enhanced drug delivery systems to various disease locations in the body.

1.6.5.2. **PSi NPs as vaccine adjuvant**

Vaccine adjuvants are defined as molecules or compounds that possess potential immunomodulatory features, and when introduced conjugated to antigen, they efficiently improve the host antigen-specific immune response [157]. One of the main targets in immunotherapies is moderating the immune responses towards pathogenic incursions and tumors. This strategy can be accomplished through prompting immune responses through appropriate delivery and presenting of antigens by engineered machines, *e.g.*, biodegradable NPs. Immunization can be achieved by antigen presenting cells (APCs), which process and present the antigen to stimulate immune response (direct approach). Alternatively, immune response can be provoked by transporting antigens to definite cellular compartments, which is followed by antigen uptake by corresponding stimulatory cells.

To deliver those antigens, PSi NPs are proposed as potential delivery carriers. Researchers from University of California have designed PSi NPs as adjuvants to deliver antigens and stimulate prospective immune responses [158]. In this study, anti-CD40

antibody was bound with PSi NPs (incorporating avidin) through biotin avidin interaction. CD40 is a co-stimulatory protein presented on APCs and is essential for their activation [159]. This anti-CD40-PSi NPs combination was found to stimulate APCs more efficient than free anti-CD40 antibody *in vitro* [158]. Accordingly, a "PSi nanovaccine" was constructed, in which, APCs targeting protein with antigen are co-incorporated into PSi NPs with anti-CD40 antibody. Through this PSi nanovaccine, immune memories can be provoked towards various antigens and multiple costimulatory molecules can be integrated into such nanovaccine. Furthermore, the fundamental photoluminescence of PS NPs enables of *in vivo* tracing.

Nonetheless, several studies have demonstrated that such NPs-based vaccines can be much more efficient than soluble peptides and protein antigens solely [160, 161], and even more adaptable and possibly safer than viral vaccines [162-164].

1.6.5.3. **PSi NPs for biomedical imaging**

Bioimaging has become an essential tool for *in vivo* and *in vitro* visualization, due to high sensitivity, dimensional resolution [165, 166]. Among biomedical imaging methodologies, PSi NPs have been given great attention due to their biocompatibility and intrinsic photoluminescence properties [165, 167].

In a study conducted by Park *et al.*, PSi NPs were tracked *in vivo*, whereas they passively accumulated in MDA-MB-435 human tumor. Measurements of the fluorescence intensity of these PSi NPs, were monitored to be decreasing correspondingly with the degradation of PSi NPs [167]. In another study Secret *et al.*, showed an enhanced cell internalization of PSi NPs functionalized with porphyrin, whereas this construction demonstrated 3-fold higher internalization to MCF-7 cells when compared to free porphyrin of equal concentration. Furthermore, this PSi NPs-porph construct possessed efficient luminescence under one photon excitation [168].

Additionally, the potential of PSi NPs to image cancer cells was demonstrated by Osminkina *et al.*, thus PSi NPs were obtained by simple mechanical grinding of PSi nanowires in water. In this study, PSi NPs achieved penetration into Hep-2 (human lung cancer) cells without significant cytotoxicity up to ~100 μg/ml. Besides, PSi NPs were

spotted to fulfill the cytoplasm of the cells displaying bright photoluminescence. They also proposed in this study, PSi NPs can be potential agents for photodynamic cancer therapies, since those NPs could photosensitize singlet oxygen generation [169]. Main advantage of PSi NPs comparing to other fluorophores is their long emission lifetime. Whereas, this long emission (5-13 μs) facilitates time-gated imaging *in vivo*. Vast imaging improvements were noticed upon administrating these PSi NPs intravenously into a mouse. Short-lived (<10 ns) emission signals due to auto-fluorescence were erased and background signals were strengthened >50-fold *in vitro* and >20-fold *in vivo* [170]. Likewise, this photoluminescence properties were enhanced when PSi NPs were functionalized through coating by bioresorbable polymers (polylactic-*co*-glycolic acid (PLGA) and polyvinyl alcohol (PVA), as reported by Gongalsky *et al.* [171].

1.6.5.4. **Other applications of PSi NPs**

PSi NPs are involved in many other applications due to their outstanding features. For instance, PSi NPs are currently involved in photodynamic therapies (PDTs) which is considered an efficient treatment for many diseases including cancers. In PDTs, PSi NPs are employed as photosensitizers, thus photoactivation with proper wavelength is applied to stimulate PSi NPs to transform to an excited state and transfer their energy (electron transfer) to the neighboring molecular oxygen, leading to production of highly cytotoxic singlet oxygen ($_1O_2$) and ROS. These formed $_1O_2$ and ROS have led to death of cancer cells either by apoptosis or necrosis [172, 173].

One more therapy using PSi NPs is thermal therapy, which use generated heat to destruct the cancer cells avoiding any drug resistance or genetic complications. As a result of the advantageous photo-thermal properties of PSi NPs, they are proposed as potential agents to absorb and transform photons to thermal energy, known as photothermal therapy (PTT). This generated heat was shown to be enough to kill 94% of cancer cells ($T = \sim 52$ °C), using PSi NPs modified with DMSO to tackle nanoparticle agglomeration [174]. Similarly, Hong *et al.*, proposed that PSi NPs combined with near-infrared (NIR) laser, were able to destroy ~93% of cancer cells *in vitro* and to remove the murine colon carcinoma (CT-26) tumors with almost no damage to the surrounding healthy tissue [175].

Overall, PSi NPs are very promising materials in nanomedicine and for the current and future scientific research. Moreover, they are becoming more widespread in various medical therapies and daily applications.

1.7. Aims of the study

As mentioned earlier, studies have presented that PSi particles tend to accumulate mainly in the liver [85, 86] upon intravenous administration. Likewise, other studies have found that after 4 h of blood injection with PSi, the particles were mainly localized in liver and spleen, while marginal accumulations were spotted in lung, heart and kidney [176, 177]. It was also reported previously that PSi NPs reactivity can alter within inflamed conditioned, *e.g.*, ROS elevated level [138].

Subsequently, in this work we aimed to investigate the behavior of PSi NPs with different surface chemistries, within acute liver inflammation environment, besides the effect of the inflammatory compounds, *e.g.*, ROS on the degradation of PSi. Viability tests were also conducted to evaluate the cellular toxicity of those PSi NPs.

In brief, our aims were as follow:

1. To investigate the immunomodulatory effect of PSi NPs within inflammatory environment, by monitoring the expression of certain pro-inflammatory cytokines in RAW macrophages cells (*in vitro*), and within acute liver inflammation (ALI) models (*in vivo*), in addition to liver function assessment through liver enzymes analysis.

2. To assess the influence of PSi NPs on ROS level within the inflammatory medium; intracellular ROS levels were monitored within RAW cells, as well as within ROS containing solution in the presence of PSi NPs.

3. To examine the PSi NPs degradation rate in ROS containing medium, via monitoring the Si content in the medium over certain time points.

4. To evaluate the toxicity of those PSi NPs and their potential to recover the viability of HepG2 liver cells under ROS-induced apoptosis conditions.

This study was conducted within a collaboration project, whereas the work was divided into two parts, *in vitro* and *in vivo.* The *in vivo* part, marked by (*) was conducted by our collaborators Yunzhan Li *et al.* from Xiamen University, China.

2. Material and methods

2.1. Fabrication of PSi

The involved PSi NPs were fabricated by electrochemical etching of monocrystalline boron-doped *p*+ type Si (100) wafers (Cemat Silicon S.A., Poland), whereas the same protocol was followed, as described in Bimbo *et al.* [178]. Thermally hydrocarbonized PSi (THCPSi) was firstly fabricated by heating at 500 °C for 15 min under 1:1 N_2-acetylene flow. Then for Un PSi production, the fabricated THCPSi films were treated in undecylenic acid at 120 °C for 16 h to obtain undecylenic acid-terminated carboxylic acid THCPSi (Un) films, as described in Jalkanen *et al.* [179]. Lastly, Un NPs were produced through wet-milling in undecylenic acid, which was centrifuged after to harvest the necessary size of NPs [178]. Thermally carbonized (TC) PSi NPs were fabricated by heating the THCPSi films absorbed with acetylene at 820 °C for 10 min, after which TC PSi NPs were harvested by wet ball milling in 1-decene [180]. Thermally oxidized (TO) PSi NPs were fabricated through placing the fresh films in atmospheric air for 2 h under 300 °C, after which the NPs were harvested by wet ball milling the TO fabricated film in EtOH [181]. Eventually, all the fabricated porous silicon nanoparticles were centrifuged and suspended in ethanol.

2.2. Characterization of PSi NPs

The NPs' size and surface zeta-potential were measured by DLS Zetasizer (Nano ZS, Malvern Instruments, UK), were samples were loaded in disposable polystyrene cuvette (SARSTEDT AG & CO., Germany) and disposable folded capillary cells (DTS1070, Malvern, UK), respectively. For each PSi NP, a stock solution was prepared in PBS 20 µg/mL, of which 20 µl was taken in 880 20 µl water for each measurement (final concentration of 0.4 µg/mL). Samples were sonicated before measuring and each measurement was done in triplicates.

The porous features were studied through N_2 adsorption/desorption method, and from the outcome data, surface area and pores characterisation of each NP was determined using Brunauer–Emmet–Teller and Barret–Joyner–Halenda theories [182]. Morphology of PSi NPs was investigated using TEM (Tecnai 12, FEI Company, USA) at acceleration voltage

80 kV. Lastly, surface properties and chemical modification were studied using FTIR with vertex 70 spectrometer (Bruker Optics, USA).

2.3. Blood analyses of acute liver inflammation (ALI) models*

Whole blood analysis was accomplished using an automatic biomedical analyzer (VetScan HM5, ABAXIS, USA), whereas manufacturers' instructions were followed. Using corresponding chemical kites for analysis, serum liver enzymes (ALP, ALT and AST) were analyzed: ALP (140318005, Mindray, China), ALT (140118005, Mindray, China), AST (140218004, Mindray, China). Then samples were prepared accordingly and measured by an automatic biomedical analyzer (BS-240vet, Mindray, China).

2.4. qPCR

Two qPCR experiments were conducted *in vitro* and *in vivo* qPCR. For *in vitro* qPCR, RAW 264.7 macrophage cells were cultured in MDEM medium and seeded in 6-well plates of $1.5\times10_5$ cells per well, whereas each group was planned in triplicates, and incubated overnight. Treated with 1 μg/mL of LPS for 4 h and washed afterwards with 1× PBS (6.7 mM, pH 7.4). PSi NPs in different concentrations were added accordingly and incubated for 3 h, after which the cells were washed again with PBS and harvested by Trypsin and total RNAs were isolated using Trizol Reagent (Magen, China).

Afterwards, corresponding cDNAs were built by the TransScript One-Step gDNA Removal and cDNA Synthesis SuperMix (Transgen Biotech, China), whereas the manufacturers' instructions were followed. cDNA was normalized against housekeeping gene glyceraldehyde-3-phosphate dehydrogenase (GAPDH), invariant endogenous gene to be used as reference gene when comparing samples together to compensate variations between samples. Lastly the qPCR step was conducted, thus the samples were amplified, and the data was analyzed through the ABI StepOnePlus Real-Time PCR System.
The primers sequences involved in the experiment were as follow:
TNF-α: 5' - CAG CCT CTT CTC ATT CCT GCT TGT G - 3', 5' -CTG GAA GAC TCC TCC CAG GTA TAT - 3'; **CXCL1**: 5' - AGC TTC AGG GTC AAG GCA AG - 3', 5' - CTG CAC CCA AAC CGA AGT - 3'; **CCL2(MCP-1)**: 5' - AGG TGT CCC AAA GAA GCT GTA - 3', 5' - ATG TCT GGA CCC ATT CCT TCT - 3'; **IL-6**: 5' - TAG TCC TTC CTA CCC CAA TTT C - 3', 5' -TTG GTC CTT AGC CAC TCC TTC - 3'; **IL-1β**: 5' -

GAA ATG CCA CCT TTT GAC AG - 3', 5' - CCA CAG CCA CAA TGA GTG AT- 3'; **GAPDH**: 5' – GCC TTC CGT GTT CCT ACC C - 3' , 5' – TGC CTG CTT CAC CAC CTT C- 3'.

For *in vivo* qPCR, 3 h after ALI establishing, two concentrations (0.3 mg/kg or 3 mg/kg) of each PSi NPs were injected intravenously, and saline was injected as control. 48 h post administration, mice were sacrificed, and liver samples were collected and kept at –80 °C for further analysis. The same qPCR protocol was followed as mentioned above.

2.5. ELISA

An *in vivo* ELISA test was conducted, whereas, all the liver specimens , which were collected and stored at –80 °C, were prepared in ice-cold saline solution before running the test. The three main cytokines of interest (TNF-α, IL-6 and IL-1β) were analyzed within the same supernatants using the mouse ELISA kit (cat. EM001, EM004, EM008 ExCell Biotech, China). Hence, the manufacturers' instructions were followed, and the corresponding absorbance were detected by Varioskan Flash Spectral Scanning Multimode Reader (Thermo Fisher Scientific, USA) at 450 nm wavelength. Lastly, the quantities of cytokines amounts were determined on standard curves of each recombinant cytokine.

2.6. Cell lines and culturing media

Two cell lines were involved in the *in vitro* studies, including murine leukemia monocyte macrophage cell line (**RAW 264.7**), and human hepatocellular carcinoma cell line (**HepG2**), whereas both of them belonged to the American type culture collection, USA. All cell lines were cultured in Dulbecco's modified Eagle's medium (DMEM, EuroClone S.p.A., Italy), consisting of 10% of fetal bovine serum (FBS) (Gibco, Invitrogen, USA), 4.5 g/L glucose, 1% nonessential amino acids, 1% L-glutamine, Pencillin (100 IU/mL), in addition to Streptomycin (100 mg/mL), all provided by HyClone, USA.

2.7. ROS consumption study

Different concentrations of each PSi NPs (10, 25, 50 and 100 µg/ml) were incubated in PBS containing 10 mM of hydrogen peroxide H_2O_2 (ROS) for 24 h under orbital agitation at 100 rpm, after which the samples were collected and centrifuged at 15000 rpm for 5

min to collect the supernatant, which were transferred afterwards in 96-well plates for further measurements. 2´,7´-dichlorodihydrofluorescein diacetate (DCF-DA) assay was used to measure ROS concentration in the samples, thus 10 μM of DCF-DA was activated (deacetylated) by incubating with 0.1 M of sodium hydroxide (NaOH) for 30 min, and then added on the samples on the 96-well plate (5 μl per well), and incubated for another 30 min.

Post incubation, DCF fluorescence in the samples was detected and measured by Varioskan Flash Spectral Scanning Multimode Reader (Thermo Fisher Scientific, USA), with excitation and emission wavelengths at 498 nm and 522 nm, respectively. Each group was done in triplicates including negative control group (no PSi NPs). DCF-DA remains nonfluorescent until the acetate groups are removed by intracellular esterase forming dichlorofluorescein, which is oxidized in the cell by peroxide H_2O_2 to form DCF fluorophore. This hydrolysis can be achieved also with NaOH. Eventually the fluorescence is measured by Varioskan.

2.8. *In vitro* ROS consumption

RAW 264.7 macrophage cells were seeded in MDEM medium in 12 well plate (5×10^5 cells per well) and kept overnight. The experiment is designed in two sets, thus in the first set, proinflammatory intracellular ROS production was stimulated by incubating the cells with 10 pg/mL of IFN-γ and 1 μg/mL of LPS for 4 h, after which the cells were washed by 1× PBS (6.7 mM, pH 7.4) to remove the traces of IFN-γ and LPS and stop their stimulation. The second set was kept without IFN-γ and LPS treatment.

Two control groups were established: blank cells and cells treated with 1 μg/mL of LPS. Then, all the cells were treated by 10 μM of DCFH-DA (0.5 mL per well) and incubated for 1 h. Afterwards, the excess of DCFH-DA was washed away through washing the cells 3 times by 1× PBS which also assure eliminating any possible traces of DCFH-DA, LPS or IFN-γ, which may affect the result.

Then PSi NPs were added to the cells in different concentrations (2, 10, 20 and 50 μg/mL) and incubated overnight. Afterwards, cells were detached and collected by 1× trypsin (0.5 ml per well), then cells were fixed in 4% of paraffinaldehyde in 1× PBS for 15 min , after

which the cells were washed by 1×PBS and stored in 4 °C for later measurement. ROS level was measured by LSR II flow cytometer (BD Biosciences, USA), using laser excitation wavelength of 488 nm and the experiment was run by FACS Diva software, whereas minimum of 5000 events were collected. Manufacturers' instructions were followed for the FACS protocol. All the groups were planned on the 12 well plates in triplicates.

2.9. HepG2 cells viability

Cell viability study was conducted in two groups, whereas the first group contained HepG2 cells cultured in MDEM medium containing different concentrations of H_2O_2 (0–2 mM), in addition to 50 μg/mL of each PSi NPs. The second group comprised HepG2 cells cultured in 0, 0.8, 1, 1.6 and 2 mM of H_2O_2 containing DMEM medium that was preincubated with 50 μg/mL of each PSi NPs for 24 h before introducing to the cells. Control sets were composed of solely HepG2 cells in DMED medium.

Both groups were incubated for 24 h, after which their cellular viabilities were measured via an ATP-luminescence assay (CellTiter-Glo® Luminescent Cell Viability Assay, Promega, USA). Manufacturer's instructions were followed, and the luminescence was detected by Varioskan Flash Spectral Scanning Multimode Reader (Thermo Fisher Scientific, USA).

2.10. PSi degradation in ROS containing medium

The experiment was designed in two groups, whereas in each group, 150 μg of each PSi NPs were incubated in 3 mL degradation medium which is composed of 1× PBS (6.7 mM, pH 7.4) containing 1% of poloxamer 188 (p188). 2 mM of 3-morpholinosydnonimine (SIN-1, Enzo Life Sciences, USA) was added to one of the two groups as ROS source, meanwhile the other group was maintained SIN-1 free.

Both groups were kept on orbital agitation of 100 rpm at 37 °C for 10 days, during which samples were collected at certain time points, and pH was monitored thoroughly. Collecting samples was performed by taking 1.2 mL of each 3 mL falcon tube to an

Eppendorf (A), then centrifuging at 13200-15000 rpm for 8 min. 1 mL of transparent supernatant was collected in another Eppendorf (B), which was filtered to a new falcon tube marked with the time point, and 4 mL of 5% nitric acid was added. Falcons containing filtered samples were sealed properly and stored at 4 °C for further measurements. 1 mL of fresh degradation medium (pre-prepared and stored in the fridge) was added to the pellet in Eppendorf A, and sonicated to recover the 1.2 mL amount. This particle solution in Eppendorf A was returned to the main falcon tubes, thus 3 mL volume in the main PSi NP falcon was maintained through the whole experiment. Control groups were set as total degradation samples of PSi NPs which were constituted by incubating PSi in NaOH solution. Eventually, all samples were measured for total Si contents by microwave plasma atomic emission spectroscopy (MP-AES, Varian Inc. Santa Clara, CA, USA).

3. Results

3.1. Characterization of PSi NPs

Three types of PSi NPs, representing the mainly applied PSi surface stabilization methods, with different surface chemistry, *i.e.*, thermally oxidized PSi NPs (TO), thermally carbonized PSi NPs (TC) and undecylenic acid modified thermal hydrocarbonized PSi NPs (Un), were included in the current study and their physiochemical characterization were correspondingly investigated. TEM was first applied to observe the morphology of these different PSi NPs (**Figure 12a**).
The hydrodynamic size and surface zeta-potential of different NPs were studied via dynamic light scattering (DLS) coupled zeta-potential analyzer. However, pore volume and pore size were studied via N_2 adsorption/desorption method, thus depending on the outcome data using Brunauer–Emmet–Teller and Barret–Joyner–Halenda theories, the specific surface area and pores characteristics were evaluated (**Figure 12b**).

Later, Fourier transform infrared spectroscopy (FTIR) was conducted to confirm the distinctive surface characteristics of those NPs. The FTIR results demonstrated distinguishable bands identified at 882 and 3740 cm^{-1}, which were attributed to $-O_ySi-H_x$ and Si-OH bonds respectively. At 1715 cm^{-1}, both Un and TO NPs showed the ν (C=O) band. Whilst, for Un NPs this band was identified as confirmation of successful undecylenic acid hydrosilylation. Meanwhile, for TC NPs, this band was attributed to the acetylene treatment and the subsequent high annealing temperature. At 1630 cm^{-1} , TO, TC and Un NPs exhibited variant hydrophobicity from this water related band, whereas it was more preeminent with TO and TC (**Figure 12c**). Although the different surface stabilizations methods executed on PSi NPs, there were hydrides remains ($-O_ySi-H_x$) detected on the surface of PSi within PSi hydride stretches area between 2100 – 2300 cm^{-1}. Despite the different surface chemistry [183], these PSi NPs shared a similar particle size, porosity and zeta-potential **Table 2**.

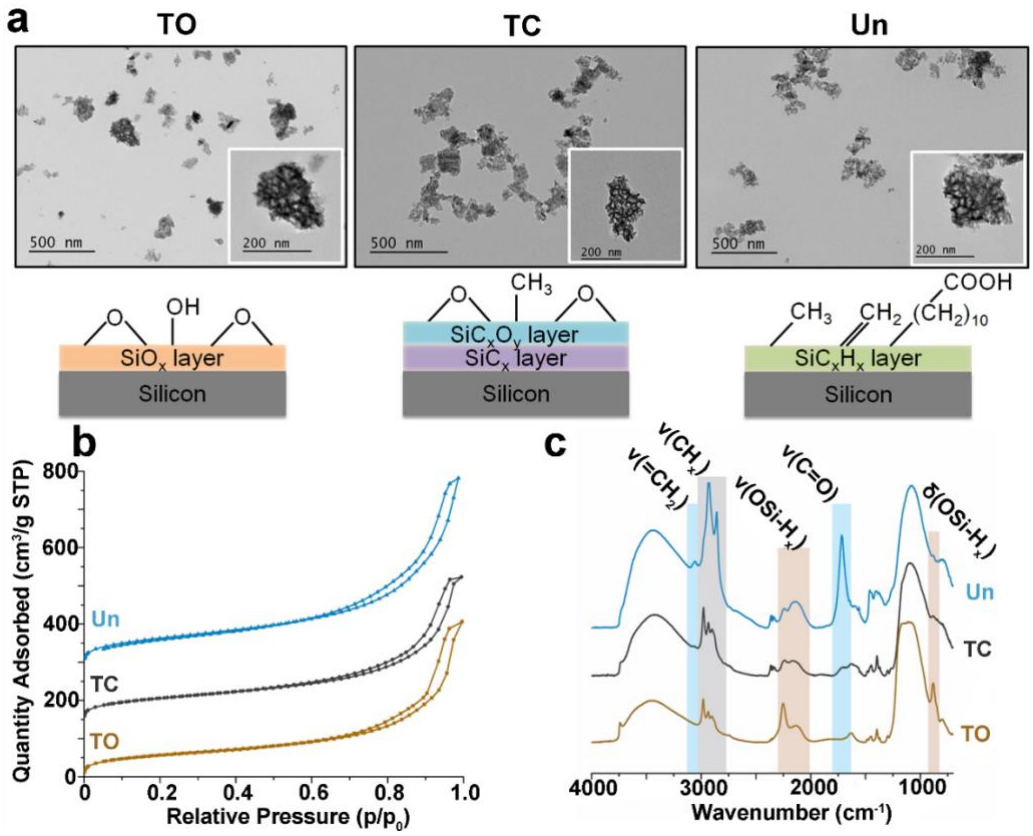

Figure 12: Physicochemical characterization of PSi NPs exhibiting the specific features of each NP, in addition to graphic illustration of their distinguished surface chemistry; thus, the morphological topographies were examined under TEM, and the result showed a great similarity in the outer appearance and diameter **(a)**. The porous properties were examined by N_2 adsorption/desorption method, which revealed UnPSi to possess the highest pore volume **(b)**. surface chemistry properties were examined by FTIR, which demonstrated the different surface chemical compositions of those PSi NPs **(c)**.

Table 2: Characterization of PSi NPs, revealed the similarity between the three PSi NPs; TO, TC and Un, whereas they shared relatively similar particles sizes, porosity and δ-surface potential.

	TO	TC	Un
Size (nm)	175 ± 15	154 ± 5	180 ± 6
δ-potential (mV)	-26 ± 2	-25 ± 5	-30 ± 1
Specific surface area (m_2/g)	203 ± 11	212 ± 4	242 ± 1
Total pore volume (cm_{-3}/g)	0.57 ± 0.04	0.52 ± 0.07	0.73 ± 0.01
Pore diameter (nm)	11.3 ± 0.2	9.9 ± 1.4	12.0 ± 0.1

3.2. Immunomodulatory influences of PSi NPs

As explained earlier, PSi NPs tended to accumulate in the liver predominantly, when injected intravenously. Besides, they also were found to exhibit altered behaviors from the inflamed environment to the healthy one. Thus, according to our goals in this study to assess the immunomodulatory effects of PSi NPs within inflammatory conditions, it was essential to induce an acute liver inflammation in mice ahead of the protocol.

3.2.1. PSi NPs within acute liver inflammation (ALI) model*

Acetaminophen (APAP) was administrated in a high dose to induce the acute liver inflammation (ALI) in the mice. APAP was reported to induce hepatocellular necrosis in 1.5 h when administrated in high dose [184]. Three hours following the induction, PSi NPs (TO, TC and Un) were introduced to ALI mice, intravenously. Each of those NPs was administrated in two concentrations, low (L) = 0.3 mg/kg and high (H) = 3 mg/kg, and saline was considered as control, whereas each group composed of 5 mice. Two groups (healthy and ALI) were left without NPs injection, which were indicated as **healthy** and **ALI** groups. After 48 h of the administration, blood samples were collected from all the groups, for further analyses.

Whole blood analyses were conducted to estimate the immunological effects of these PSi NPs and the success of establishing the ALI models, represented in the total number of the white blood cells (WBCs). The result showed that **ALI** groups exhibited a statistically significant ($p = 0.013$) increase in WBCs level, when compared with the **healthy** groups, which is a confirmatory sign of establishing the ALI model [185]. Nevertheless, there was no further significant increase of WBCs triggered by introduced PSi NPs, when compared with ALI group. Thus, introducing either of these PSi NPs did not promote any further inflammatory effect.

Afterwards, the compositions of WBCs in the blood were analyzed in all of the groups, meaning; the ratio of the main three WBCs types: Granulocytes (GRA), **Figure 13b**; Monocytes (MON), **Figure 13c**; and Lymphocytes (LYM), **Figure 13d.** Likewise, the outcome showed that administration of any of these PSi NPs did not exhibit any further alteration of the overall composition of WBCs, upon with the ALI group. This reading

endorses the insignificant effect of these PSi NPs on the immune system in either healthy or inflamed environments.

Afterwards, the influence of PSi NPs on liver functions was examined through serum analysis. Alanine aminotransferase (ALT), aspartate aminotransferase (AST) and alkaline phosphatase (ALP) is defined as universal indicators for the liver functions [186], thus the measurements of those enzymes were analyzed to assess the progression of the consequent hepatocellular necrosis. From the result, it was distinguished that PSi NPs had a burlier influence on AST than ALT. Except of TC H group, AST level were declined with most of the introduced PSi NPs, while a limited effect was noticed on ALT level comparing to ALI group **Figures 13f and 13e,** concluding that most of PSi NPs led to reduced AST/ALT value, of which, Un H group presented the most statistically significant decrease (**Figure 13g**). Likewise, Un H group showed a similar decreasing effect on ALP value when compared to ALI group (**Figure 13h**)**.** This distinguished decline in AST/ALT and ALP level, can be translated as indicators for improving inflammation conditions and liver necrosis mend [187].

Glutathione (GSH) is an important antioxidant whose deficiency has been attributed to liver malfunction [188]. Therefore, GSH level was further analyzed as confirmatory assessment of the effect of PSi NPs on the ALI mice. Captivatingly, ALI mice showed improved GSH level after administrating TO H and Un H groups (**Figure 13i**), ($p = 0.032$ for TO H and $p = 0.019$ for Un H.

Collectively, the enhanced values of AST/ALT, ALT and GSH in ALI group may refer to potential ability of PSi NPs to mitigate the inflammation conditions.

3.2.2. *In vitro* and *in vivo** effects of PSi NPs on the proinflammatory cytokines

Under pathological circumstances, the inflammation is accompanied by elevated values of the proinflammatory cytokines, which can induce perilous consequences [189]. And since PSi NPs showed enhancing effect on liver function, it is beneficial to evaluate the immunomodulatory effect of those NPs and their influence on the proinflammatory cytokines. Therefore an *in vivo* study was resumed to assess the immunomodulatory

effect of these PSi NPs, utilizing quantitative real-time polymerase reaction (qPCR) to quantitively analyze mRNA level of those corresponding proinflammatory cytokines within samples from both healthy and ALI groups, in order to evaluate the inflammatory progression after injecting the PSi NPs. In order to conduct qPCR, corresponding primers of each cytokine were engaged to construct and amplify the consequent cDNA strands.

The main emphasized cytokines analyzed in this *in vivo* study are: interleukin 1 beta (IL-1β), Interleukin 6 (IL-6), tumor necrosis factor α (TNF-α), chemokine (C-X-C motif), ligand 1 (CXCL-1), chemokine (C-C motif) and ligand 2 (CCL-2).

The result proposed that mice in ALI group demonstrated elevated values: 3.3-folds, 2.7-folds, 2.9-folds, 2.8-folds and 4.9-folds of TNF-α, IL-6, IL-1β, CCL-2 and CXCL-1, respectively, comparing to healthy mice. Remarkably, administrating PSi NPs exhibited surface chemistry reliant immunoregulatory effect on ALI mice, however, TO H and Un H exhibited dramatically decreased level of TNF-α and IL-6 expression, in addition to lower IL-1β expression in Un H as well. Again, both of TC groups did not present any significant variation (**Figure 14a**).

This was followed up by an enzyme linked immunosorbent assay (ELISA) to quantitively measure these three cytokines (TNF-α, IL-6 and IL-1β) in the liver. ALI mice exhibited escalated amount (3.2-folds, 1.3-folds and 1.4-folds) of TNF-α, IL-6 and IL-1β, respectively, when compared to healthy group. However, TO and Un reduced the amount of these proinflammatory cytokines in concentration related approach. Regarding TC groups, an indistinct effect was observed, whereas at TC low concentration, IL-1β amount was slightly decreased, meanwhile at TC high concentration, TNF-α amount was mildly decreased (**Figure 14b-d**). These immunomodulatory effect on the proinflammatory cytokines, after PSi NPs administration, may explain the inflammation enhancements and relieving effect of PSi NPs.

Next, *in vitro* study was conducted to confirm the obtained *in vivo* results, whereas capability of PSi NPs was examined to induce production of any proinflammatory cytokines when administrated solely to healthy lab cultured macrophages. Therefore, Murine macrophage cell line RAW 264.7 were cultured overnight in Dulbecco's modified Eagle's medium (DMEM) containing 10% of healthy mice plasma (further

referred as healthy medium). Cells were treated with 1 μg/mL of LPS for 4 h, to activate those macrophages to express the cytokines of interest, and two **control** groups were set; positive control, and negative control, which was treated only with DMEM medium without PSi NPs. Afterwards, the cells were washed by PBS and PSi NPs were added in the two concentration: low = 2 μg/mL and high 20 μg/mL. Finally, the mRNA was extracted, and qPCR was conducted to evaluate the cytokines expression in the cells. Thus, the corresponding primers of the cytokines were employed to construct and amplify the consequent cDNA strands.

The result suggested that most of introduced PSi NPs did not significantly provoke any further cytokines production except TO (high concentration), which slightly activated RAW macrophages (**Figure 15**).

This result suggested the biocompatibility of most of administrated PSi NPs and their diminutive influence to induce potential immune-inflammatory response, which encourages additional studies to further understand PSi NPs reactivity and behavior within biological environment.

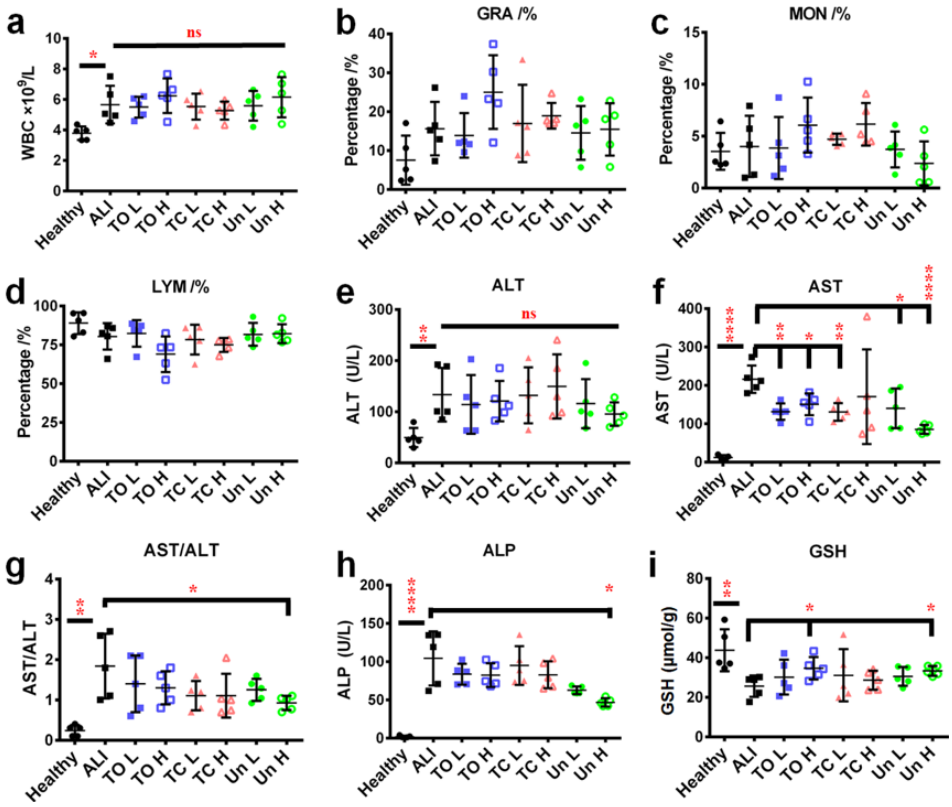

Figure 13: The altered physiology of diseased liver after *in vivo* administrating PSi NPs. Upon establishing ALI model by APAP and administrating different concentrations of PSi NPs 3 h after (L = 0.3 mg/kg, H= 3 mg/kg), a whole blood analysis was conducted after 48 h for reviewing the biological changes within the ALI models. The outcome results proposed the following potential events: **(a)** WBCs number in ALI model was not significantly affected by administration of PSi NPs, neither the composition of the main WBCs types; granulocytes (**b)**, monocytes **(c)** and lymphocytes **(d)** with exception of TO NPs **(h)**, which exhibited slightly increase of GRA and MON. For Liver enzymes' analysis, administration of PSi NPs did not affect ALT values **(e)** but decreased AST significantly **(f)**, *i.e.*, TO H ($p = 0.0124$), TO L ($p=0.0019$), TC L ($p = 0.0020$), Un H ($p < 0.0001$) and Un L ($p = 0.027$). These changes were concluded in altered AST/ALT value, subsequently, with Un H reaching statistical significance of $p= 0.038$ **(g)**. Likewise, Un H group exhibited significant decrease of ALP ($p= 0.0070$) **(i)**. lastly, GSH value was noticeably enhanced within TO H ($p=0.032$) and Un H ($p=0.019$) groups.

The data on the graphs are plotted as mean ± SD obtained from 5 neutral duplicates, *$p < 0.05$, **$p < 0.01$, ***$p < 0.0005$ and ****$p < 0.0001$ correlated to ALI model (two-tailed Student's *t* test).

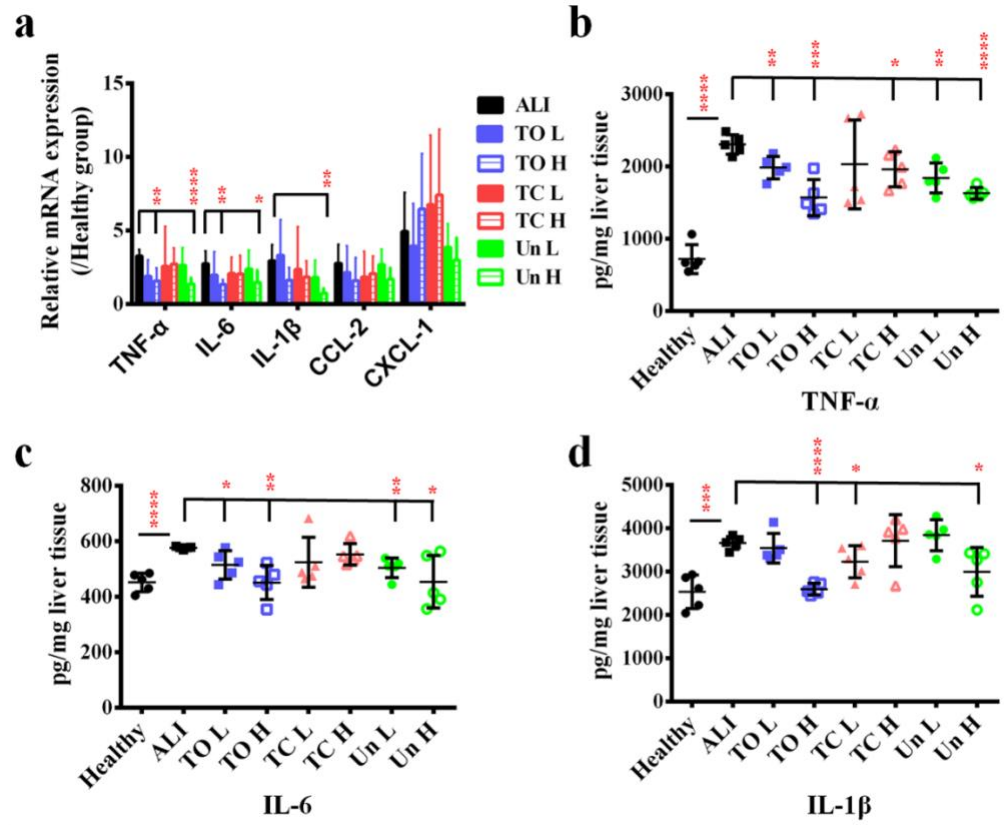

Figure 14. ***In vivo*** **immune response in ALI models upon administrating PSi NPs.** After establishing ALI model and introducing PSi NPs, as mentioned in Figure 13, mRNAs of proinflammatory cytokines were detected by qPCR **(a)**, whereas mRNA level of each cytokine from healthy mice was set at 1. Comparing to ALI, group, TNF-α and IL-6 expressions were decreased in both groups TO H (TNF-α, $p = 0.0048$ - IL-6, $p = 0.0096$), and Un H (TNF-α, $p < 0.0001$- IL-6, $p = p = 0.044$). In addition to dropped expression of IL-1β in Un H group ($p = 0.0025$).
This qPCR was followed by ELISA for quantification of these cytokines, whereas more precise effects were detected. **(b)** TNF-α expression was significantly inhibited by PSi NPs when compared to ALI group; TO H ($p = 0.004$), Un H ($p < 0.0001$), Un L ($p = 0.0031$), TC H ($p = 0.025$), TO L ($p = 0.0083$). **(c)** likewise, IL-6 expression was affected by introducing PSi NPs, whereas comparing to ALI groups, the expression levels were less in TO H ($p = 0.0019$), Un H ($p = 0.020$), Un L ($p = 0.0019$), TO L ($p = 0.029$) groups. **(d)** PSi NPs effect on IL-1β expression, was monitored , thus TO H exhibited the greatest reducing effect ($p < 0.0001$), followed by Un H ($p = 0.033$) and TC L ($p = 0.041$).

- The data on the graphs are plotted as mean ± SD obtained from 5 neutral duplicates, *$p < 0.05$, **$p < 0.01$, ***$p < 0.0005$ and ****$p < 0.0001$ correlated to ALI model (two-tailed Student's *t*-test).

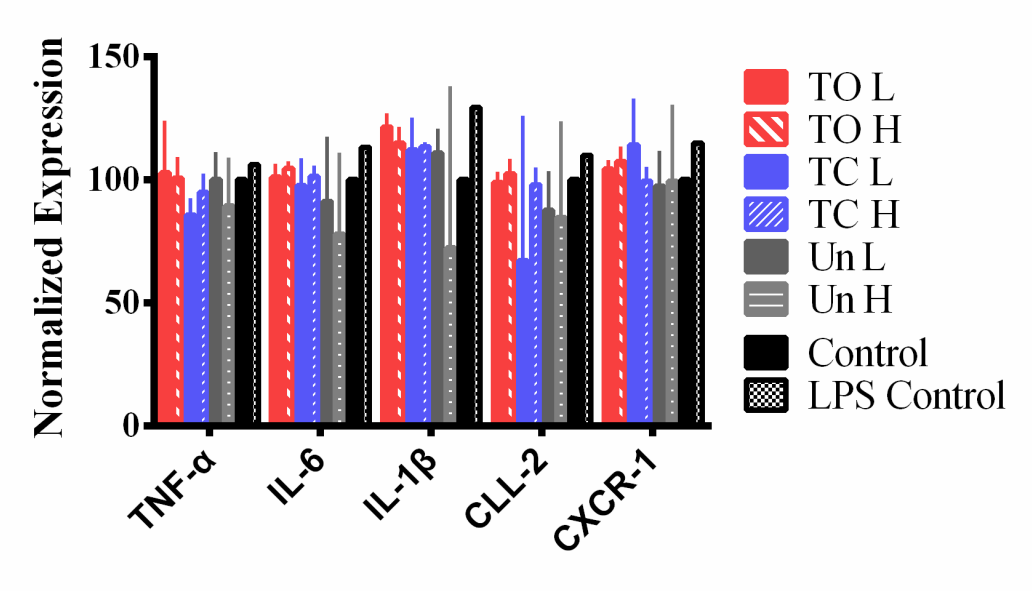

Figure 15. ***In vitro*** **qPCR revealing the immunomodulatory effects on inflamed macrophages upon introducing PSi NPs**. Inflammation was provoked in RAW cells with 1 μg/mL LPS for 4 h, after which PSi NPs (L = 2 μg/mL and H = 20 μg/mL) were introduced. The qPCR results proposed the PSi NPs to possess relatively neutral immuno-effect, whereas most of the cytokines were not significantly further induced by introducing PSi NPs. Nevertheless, some PSi NPs reduced some cytokines expressions, e.g., Un H decreased IL-1β, IL-6 and CCL-2.

3.3. PSi NPs modulation effect on intracellular ROS

As explained earlier that ROS compounds are critical co-inflammatory product that provoke further damage and even cell death eventually, in addition to reported mitochondria damage vastly correlated to escalated generation of ROS [190]. AST increasing level upon creating ALI model, may be considered a strong proof of mitochondrial damage, based on fact that AST predominantly exist in the mitochondria. Hence, ROS is another crucial prospective to investigate within the inflammation environment. Moreover, several previous studies have demonstrated the chemical reactivity of PSi material with ROS due to the reductive nature of PSi. Notwithstanding the surface stabilization modifications, the main structure of PSi NPs backbone is remained composed of Si-Si bonds which tend to react with ROS compound, within an oxidation reaction, to build Si-O-Si bonds which assist the hydrolysis and depletion of the PSi NPs (**Figure 16a**) [138]. Thus, it is anticipated that administration of PSi NPs may have some potential influence on the ROS level which may relief the oxidative stress and mitigate inflammation, eventually.

Firstly, we assessed the PSi NPs capability to consume ROS due to the prementioned reactivity. Therefore, PSi NPs in different concentrations were incubated with ROS (H_2O_2) overnight, after which the ROS levels in the media were measured (**Figure 16e**).

The result demonstrated that ROS consumption occurred in concentration dependent routine. TO has expressed the highest consuming capability while Un had minor effect, and TC was located between TO and Un. We suggested this phenomenon has happened in such manner, due to the different surface chemistry of these three PSi NPs that can affect the hydrophilicity of this NPs to the watery incubation solution, which obviously can restrain the reactivity [191]. Subsequently, this was confirmed by wetting contact angle (WCA) study, by installing a 5 µL water droplet on glass slide enclosed by dried PSi NPs film. After this, the contact angle between the water drop and PSi NPS films was examined with attension theta optical tensiometer. Unsurprisingly, TO has exhibited the highest hydrophilicity, meanwhile Un showed the lowest: TO 51° ± 5°, TC 62° ± 4° and Un 122° ± 6° (**Figure 17**).

Thereafter, *in vitro* study was established to evaluate the effect of PSi NPs on intracellular ROS of cultured Murine macrophages RAW 264.7. ROS level was monitored under both healthy and inflammatory conditions, whereas LPS and interferon γ (IFN-γ) were introduced to RAW cells to activate/induce inflammation. ROS levels was detected by 2',7'-dichlorodihydrofluorescein diacetate (DCFH-DA) fluorescence assay [192]. Upon introducing TO, TC and Un PSi NPs to healthy RAW cells, there was no influence recorded on the intracellular ROS, regardless of PSi NPs concentrations (**Figure 16c**). This result was confirmed from previous study that demonstrated PSi NPs scarcely elevated the intracellular ROS level within macrophages, under healthy conditions [192]. However, under inflammatory conditions and elevated proinflammatory ROS production within RAW macrophages (above 2-fold), because of adding LPS and IFN-γ, administrating PSi NPs did not present distinguished effect on intracellular ROS, neither further increasing nor decreasing (**Figure 16d**).

Remarkably, this result revealed the restricted influence of PSi NPs on the intracellular ROS within cellular environment. However, this needed to be confirmed by viability test to investigate any interfering influence of PSi NPs on the cellular viability, which may impact the overall intracellular ROS level.

3.4. Cellular viability reverse effects by PSi

The preceding experiment was followed by this study to assess the ability of PSi NPs to prevent cell apoptosis provoked by ROS (H_2O_2). HepG2 liver carcinoma cells were cultured and incubated with different concentrations of H_2O_2, in addition to 50 μg/mL of each PSi NPs type, for 24 h. Upon examining the cell viability after 24 h, no enhancement on cell viability was observed (**Figures 17g and 17h**). However, when PSi NPs were incubated with H_2O_2 for 24 h before administrating to HepG2 cells, only TO PSi NPs were observed to slightly mitigate the toxicity of H_2O_2 and recover ROS induced cellular apoptosis (**Figure 16f**). This phenomenon can propose that H_2O_2 provoked cellular apoptosis occurred in faster rhythm than ROS consumption by PSi NPs, which corresponds to the result concluded from previous study by Liu *et al.* [193].

The overall result refers to the *in vitro* limited effect of PSi NPs to consume ROS within cellular conditions, thus failing to mitigate the inflammatory condition. In addition, it demonstrates the biocompatibility of those PSi NPs, which did not exhibit any significant cellular toxicity.

Nevertheless, these PSi NPs are influenced by ROS within oxidation reaction in favor of enhanced degradation. For further understanding of this ROS induced PSi NPs degradation, we conducted the following degradation experiment.

3.5. Effect of ROS in modulating PSi degradation

As explained earlier, one of the preferred characteristics of the biomaterial is to be degradable and eradicable from the biological system after their function is accomplished, because it has been found in previous studies that prolongated incubation time of the biomaterial may consequence into long-lasting inflammation [109, 138]. Moreover, the microenvironment surrounding the NPs may have an effect on their degradation manner, which has been presented in some publications that under inflammatory conditions, the microenvironment exhibited an expediting influence on the *in vivo* degradation demeanour of PSi microparticles [138]. Subsequently, here we investigated the influence of the proinflammatory ROS compounds, which occur abundantly within the inflamed area, on PSi NPs degradation routine. Thus, we incubated H_2O_2, as ROS source, with different concentrations of the three PSi NPs particles; TO, TC and Un, whereas ROS

concentration was monitored periodically, through 2´,7´-dichlorodihydrofluorescein diacetate (DCF-DA) fluorescence assay.

Interestingly, ROS concentration and PSi NPs concentrations exhibited inverse proportionality relationship, whereas ROS concentration was decreasing correspondingly with the increase of PSi NPs concentration (**Figure 16e**). More precisely, TO PSi NPs displayed the most capability to consume ROS, meanwhile, the effect of Un PSi NPs was scarcely noticed. TC PSi NPs came between TO and Un to affect ROS concentration.

This result can be attributed to the contrasting surface chemistry of these PSi NPs, which conflicts with surface wetting procedure, because TC and Un possess hydrophobic surfaces, as exhibited earlier in the previous FTIR study and WCA study (**Figures 12c and 16**), respectively.

This study was followed by measuring the degradation manner of those PSi NPs in presence and absence of different ROS (3-morpholinosydnonimine (SIN-1)). Samples were collected frequently based on specific timeline and total Si-content was analyzed in each sample by microwave plasma atomic emission spectroscopy.

Similarly, the degradation rate was noticeably increased in presence of ROS in varied magnitudes (**Figure 16b**), and TO showed an accelerated degradation rate when ROS added, whereas the effect was noticed during the first 6h of incubation. In addition, it took longer time for TC and Un to show enhanced degradation with ROS, whereas the effect on TC was not observable until the second day, meanwhile Un showed a boosted degradation only after 7 days.

This behavior reconfirms that different surface chemistry of these PSi NPs, as well as the hydrophobicity may limit the reactivity of ROS with the silicon bonds. ROS can accelerate the degradation of PSi NPs through oxidizing the Silicon bonds (Si-Si), however, the time required to expose these silicon bonds is highly dependent on the variant surface chemistry and hydrophobicity of these particles.

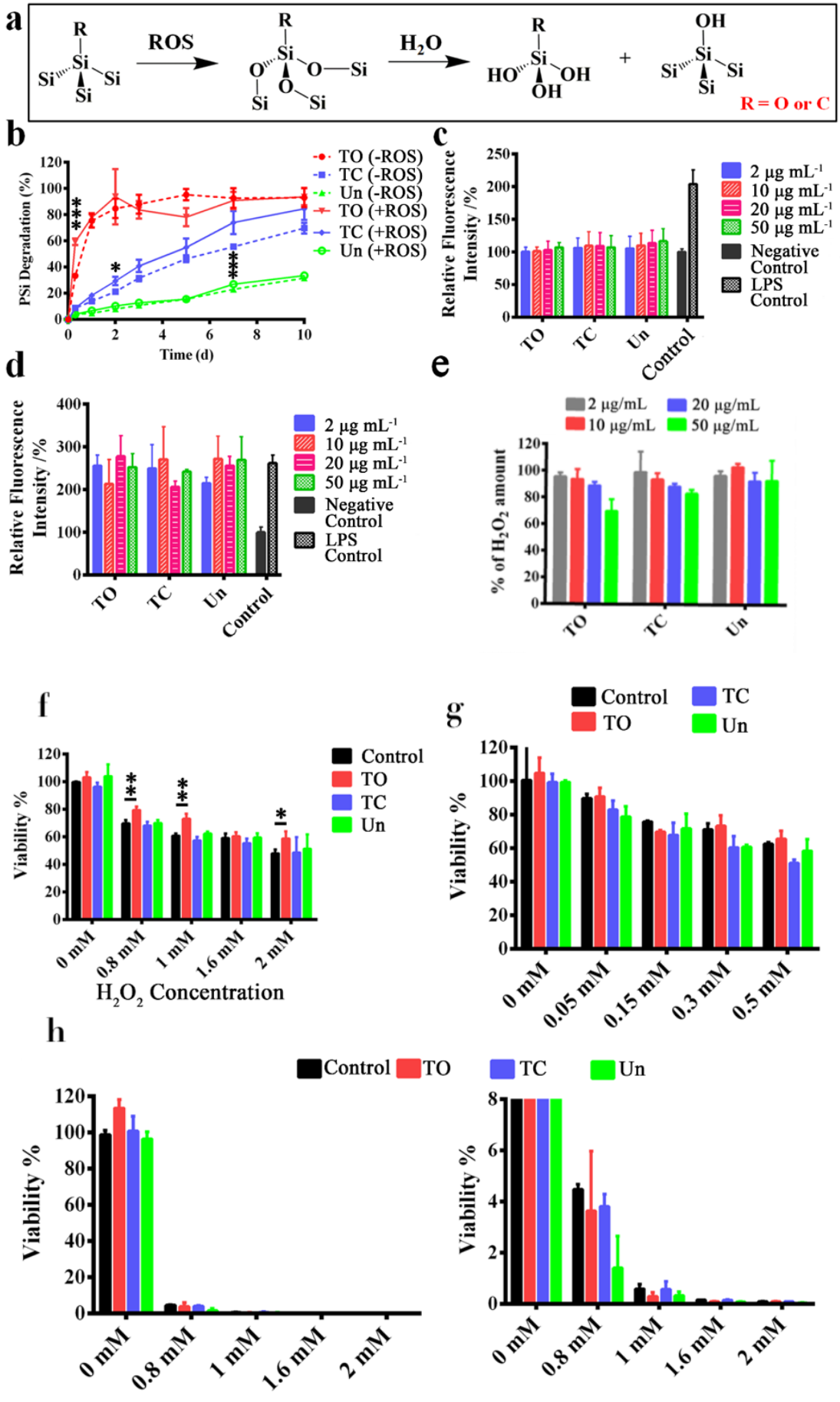
a
ROS
H_2O
R = O or C
b
PSi Degradation (%)
Time (d)
TO (-ROS)
TC (-ROS)
Un (-ROS)
TO (+ROS)
TC (+ROS)
Un (+ROS)
c
Relative Fluorescence Intensity /%
2 μg mL-1
10 μg mL-1
20 μg mL-1
50 μg mL-1
Negative Control
LPS Control
TO
TC
Un
Control
d
Relative Fluorescence Intensity /%
e
% of H_2O_2 amount
2 μg/mL
10 μg/mL
20 μg/mL
50 μg/mL
f
Viability %
Control
TO
TC
Un
0 mM
0.8 mM
1 mM
1.6 mM
2 mM
H_2O_2 Concentration
g
Viability %
0 mM
0.05 mM
0.15 mM
0.3 mM
0.5 mM
h
Viability %
0 mM
0.8 mM
1 mM
1.6 mM
2 mM

Figure 16. ROS compounds are inflammation co-product causing an oxidative stress and chemically it tends to react with PSi NPs, more specifically with the Si-Si bonds, in an oxidation reaction. This reaction results into Si-O-Si forms which is more degradable in presence of H_2O **(a)**. PSi NPs occurring in ROS containing medium would exhibit an accelerated degradation **(b)** due to the previous mentioned reaction. Whereas upon incubating 50 µg/mL of PSi NPs in PBS medium containing ROS source (2 mM of SIN-1), this phenomenon was more noticeable with TO and TC than Un, which is attributed to the variant surface chemistry of those PSi NPs.
This was followed by another study to evaluate PSi NPs effect on ROS compounds within intracellular environment, thus PSi NPs (2-50 µg/mL) were incubated for 24 h with two sets of RAW cells, **(c)** healthy RAW set and **(d)** inflamed RAW cells set (inflammation was established through incubating cells with 1 µg/mL of LPS and 10 pg/mL of IFN-γ for 4 h). Nevertheless, two control groups were maintained for both sets; negative control and positive control (LPS 1 µg/mL). When intracellular ROS levels were monitored in both sets, PSi NPs did not exhibit any significant effect of ROS level in either healthy or inflamed RAW cells.
(e) ROS consuming properties was examined through incubating different concentrations of PSi NPs (2-50 µg/mL with 1 mM of H_2O_2 for 24 h, after which, the remaining ROS concentration was determined by DCFH-DA assay. The result proposed TO PSi to have the strongest ROS consuming effect followed by TC and Un. However, the ROS consumption occurred in a concentration dependent manner.
(f) PSi NPs were tested for their ability to recover cell viability and reverse ROS induced apoptosis, thus HepG2 cell line was involved. PSi NPs (50 µg/mL) were incubated in H_2O_2 containing DMEM medium (0-2 mM) for 24 h before introducing to HepG2 cells. TO PSi NPs exhibited a potential effect to recover the cellular viability. Nevertheless, when same experiment was conducted without preincubation of PSi NPs with H_2O_2, there was no significant recovery effect recorded on cellular viability when after introducing PSi NPs **(g,h)**.

The data on the graphs are plotted as mean ± SD obtained from 3 duplicates, *$p < 0.05$, **$p < 0.01$, ***$p < 0.0005$ and ****$p < 0.0001$ correlated to ALI model (two-tailed Student's *t*-test).

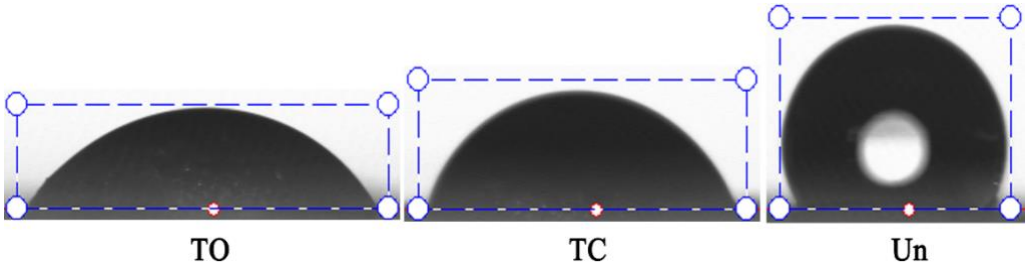

Figure 17. Evaluating the WCA of the involved PSi NPs (TO, TC and Un). Un exhibited the highest hydrophobicity, while TO demonstrated the highest hydrophilicity. TO 51° ± 5°, TC 62° ± 4° and Un 122° ± 6°.

4. Discussion

Nowadays, PSi materials are widely abundant within biomedical applications for various purposes, including drug delivery, diagnostics and immunotherapy, due to their high biodegradability in the physiological environment and effortless modifications of their physicochemical and biophysical properties. Nevertheless, further researches are still required for better understanding about the reactivity of these materials with the body biology.

As demonstrated earlier, immune responses to NPs may highly depend on protein corona accumulated around the NPs' core [69, 77-82]. However, in this study we have investigated the consequential events occur upon introducing those NPs to the body, during a nanomedical therapy, for instance, rather than examining the structure of protein corona. And since the liver is a main ultimate harbor for NPs accumulation, it was considered to be a suitable example to study the *in vivo* alterations arisen upon administrating NPs.

Firstly, the three surface chemistries modified PSi NPs were characterized and their surfaces were distinguished to assure the surface chemistry modifications, as well as the physicochemical properties. Whereas, they all exhibited similar particle size, porosity and zeta-potential, nevertheless, FTIR result demonstrated their distinctive surface chemistry.

When investigating liver functions after introducing the PSi NPs, Un and TO PSi NPs presented a promising aptitude to improve inflammation conditions of necrosing liver, which was recognized by improved AST/ALT and GSH values. Moreover, those PSi NPs did not provoke any significant immune response whereas the WBCs level and compositions was not altered after introducing the PSi NPs.

Nevertheless, it has been insinuated in earlier studies, that Un PSi NPs exhibited a slight toxicity on the liver when administrated under normal physiological circumstances, because it was accompanied by diminutive increase in serum lactate dehydrogenase (LDH) and AST levels. Meanwhile, TO and TC PSi NPs revealed satiated biocompatibility under same conditions [192, 194]. In addition, in the current study we demonstrated that these three PSi NPs did not stimulate any further hepatic inflammation

when administrated under ALI conditions, and that TO and Un exhibited aptitude to mitigate the liver injury. Both results together can be concluded that PSi NPs behave differently under ALI conditions when compared to normal states, and this behavior can be attributed to the variant surface features of the PSi NPs.

Similarly, *in vivo* results showed TO and Un PSi NPs were able to decrease inflammatory cytokines; decreased level of TNF-α and IL-6 expression in TO H and Un H groups, and dropped IL-1β expression in Un H. Moreover, those PSi NPs did not provoke significant cytokines production when introduced to RAW cells *in vitro*, with exception of TO H, where macrophages were slightly activated. Interestingly, these results may match with some previous studies presented that oxidized PSi NPs (*e.g.*, TO) had a provoking effect on the immune system, whereas they were able to activate the maturations of the DCs and assisted proliferation and differentiation of lymphocytes. In addition, TC and Un had a very limited effect on the immune response [142, 144]. Nevertheless, this can be attributed to the fluctuating behavior of those NPs that can vary within the same inflammatory environment that rises to different biological outcome.

Even though, TO and Un PSi NPs have exhibited a denoted effect on proinflammatory cytokines, none of the PSi NPs have demonstrated a significant effect on intracellular proinflammatory ROS. Nevertheless, the interaction between Si-Si bonds, in the PSi NPs backbones, and ROS compounds was confirmed. Furthermore, ROS consumption has been demonstrated to improve the degradation process of PSi NPs dramatically, TO in particular. However, these phenomena were not of much efficiency *in vitro.*

5. Conclusions

In this study, the biological influence of variant surface chemistries of PSi NPs was demonstrated on several perspectives, *i.e.*, immune response, inflammatory mitigation and cellular interaction. Besides, the effect of the surrounding environment on the behavior of PSi NPs, *e.g.*, degradation.

Although, minor immune responses were detected, those investigated PSi NPs did not demonstrate significant cellular toxicity, but exhibited a promising potential to improve and attenuate the inflammatory conditions. Furthermore, these PSi NPs exhibited a potential consumption capacity of proinflammatory ROS compounds, which were founds to boost the degradation process of PSi NPs, proposing an improved biodegradability and clearance.

Nevertheless, there is more investigations required to further understand the mechanisms and reactions of these PSi NPs and the functionality of their protein corona within cellular environment.

6. References

1. López-Serrano, A., et al., *Nanoparticles: a global vision. Characterization, separation, and quantification methods. Potential environmental and health impact.* Analytical Methods, 2014. **6**(1): p. 38-56.
2. Khan, I., K. Saeed, and I. Khan, *Nanoparticles: Properties, applications and toxicities.* Arabian Journal of Chemistry, 2019. **12**(7): p. 908-931.
3. Alexis, F., et al., *Factors Affecting the Clearance and Biodistribution of Polymeric Nanoparticles.* Molecular Pharmaceutics, 2008. **5**(4): p. 505-515.
4. Jain, P.K., et al., *Calculated Absorption and Scattering Properties of Gold Nanoparticles of Different Size, Shape, and Composition: Applications in Biological Imaging and Biomedicine.* The Journal of Physical Chemistry B, 2006. **110**(14): p. 7238-7248.
5. Jain, P.K., I.H. El-Sayed, and M.A. El-Sayed, *Au nanoparticles target cancer.* Nano Today, 2007. **2**(1): p. 18-29.
6. Chen, C., et al., *Multihydroxylated [Gd@C82(OH)22]n Nanoparticles: Antineoplastic Activity of High Efficiency and Low Toxicity.* Nano Letters, 2005. **5**(10): p. 2050-2057.
7. Hajipour, M.J., et al., *Antibacterial properties of nanoparticles.* Trends in Biotechnology, 2012. **30**(10): p. 499-511.
8. AshaRani, P.V., et al., *Cytotoxicity and Genotoxicity of Silver Nanoparticles in Human Cells.* ACS Nano, 2009. **3**(2): p. 279-290.
9. Yin, Q., et al., *Glucose-assisted transformation of Ni-doped-ZnO@carbon to a Ni-doped-ZnO@void@SiO2 core–shell nanocomposite photocatalyst.* RSC Advances, 2016. **6**(45): p. 38653-38661.
10. Qu, Z., et al., *Microstructure and Characteristic of BiVO4 Prepared under Different pH Values: Photocatalytic Efficiency and Antibacterial Activity.* Materials, 2016. **9**(3).
11. Pant, H.R., et al., *Antibacterial and photocatalytic properties of Ag/TiO2/ZnO nano-flowers prepared by facile one-pot hydrothermal process.* Ceramics International, 2013. **39**(2): p. 1503-1510.
12. Akhavan, O., et al., *CuO/Cu(OH)2 hierarchical nanostructures as bactericidal photocatalysts.* Journal of Materials Chemistry, 2011. **21**(26): p. 9634-9640.
13. Rushton, E.K., et al., *Concept of Assessing Nanoparticle Hazards Considering Nanoparticle Dosemetric and Chemical/Biological Response Metrics.* Journal of Toxicology and Environmental Health, Part A, 2010. **73**(5-6): p. 445-461.
14. Nel, A., et al., *Toxic Potential of Materials at the Nanolevel.* Science, 2006. **311**(5761): p. 622-627.
15. Ju-Nam, Y. and J.R. Lead, *Manufactured nanoparticles: An overview of their chemistry, interactions and potential environmental implications.* Science of The Total Environment, 2008. **400**(1): p. 396-414.
16. Cashin-Garbutt, *Nanomedicine – Past, Present and Future*, in *News-Medical.* 2019, January 22.
17. Narayan, R., et al., *Mesoporous silica nanoparticles: A comprehensive review on synthesis and recent advances.* Pharmaceutics, 2018. **10**(3): p. 118.
18. Mohan Bhagyaraj, S. and O.S. Oluwafemi, *Chapter 1 - Nanotechnology: The Science of the Invisible*, in *Synthesis of Inorganic Nanomaterials*, S. Mohan Bhagyaraj, et al., Editors. 2018, Woodhead Publishing. p. 1-18.

19. Feynman, R.P., *There's plenty of room at the bottom [data storage].* Journal of Microelectromechanical Systems, 1992. **1**(1): p. 60-66.
20. Moghimi, S.M., A.C. Hunter, and J.C. Murray, *Nanomedicine: current status and future prospects.* The FASEB Journal, 2005. **19**(3): p. 311-330.
21. Heera, P. and S. Shanmugam, *Nanoparticle characterization and application: an overview.* Int. J. Curr. Microbiol. App. Sci, 2015. **4**(8): p. 379-386.
22. Wang, M.D., et al., *Nanotechnology for targeted cancer therapy.* Expert Review of Anticancer Therapy, 2007. **7**(6): p. 833-837.
23. Pilkington, A., L.L. Lee, and C.K. Chan. *Defining Key Inventors: A Comparison of Fuel Cell and Nanotechnology Industries*. in *PICMET '07 - 2007 Portland International Conference on Management of Engineering & Technology*. 2007.
24. Chan, W.C.W. and S. Nie, *Quantum Dot Bioconjugates for Ultrasensitive Nonisotopic Detection.* Science, 1998. **281**(5385): p. 2016-2018.
25. Wang, J., et al., *Electrochemical stripping detection of DNA hybridization based on cadmium sulfide nanoparticle tags.* Electrochemistry Communications, 2002. **4**(9): p. 722-726.
26. Pantarotto, D., et al., *Immunization with Peptide-Functionalized Carbon Nanotubes Enhances Virus-Specific Neutralizing Antibody Responses.* Chemistry & Biology, 2003. **10**(10): p. 961-966.
27. Bowman, K. and K.W. Leong, *Chitosan nanoparticles for oral drug and gene delivery.* Int J Nanomedicine, 2006. **1**(2): p. 117-28.
28. Nam, J.-M., C.S. Thaxton, and C.A. Mirkin, *Nanoparticle-Based Bio-Bar Codes for the Ultrasensitive Detection of Proteins.* Science, 2003. **301**(5641): p. 1884.
29. Y. Lin, J.W., H. Wang, H. Wu and Z. Tang, *Chemical Sensors 8: Chemical Sensors and Analytical Systems.* ECS Transactions, ed. R. Mukundan, et al., 2008. **vol. 16:11**: p. pp. 477–482.
30. Mahtab, R., J.P. Rogers, and C.J. Murphy, *Protein-Sized Quantum Dot Luminescence Can Distinguish between "Straight", "Bent", and "Kinked" Oligonucleotides.* Journal of the American Chemical Society, 1995. **117**(35): p. 9099-9100.
31. Wang, L., Zhang, J., Wang, X. et al., *Gold nanoparticlebased optical probes for target-responsive DNA structures.* Gold Bull, 2008.
32. Perez, J.M., et al., *Viral-Induced Self-Assembly of Magnetic Nanoparticles Allows the Detection of Viral Particles in Biological Media.* Journal of the American Chemical Society, 2003. **125**(34): p. 10192-10193.
33. Santos, H.A., et al., *Porous silicon nanoparticles for nanomedicine: preparation and biomedical applications.* Nanomedicine, 2014. **9**(4): p. 535-554.
34. Kroto, H.W., et al., *C60: Buckminsterfullerene.* Nature, 1985. **318**(6042): p. 162-163.
35. Louazri, L., et al., *Study of the Effect of Substitution on Phtalocyanine Based Compounds for Photovoltaic Application.* International Journal of Chemistry and Materials Research, 2015. **3**: p. 65-78.
36. Friedman, S.H., et al., *Inhibition of the HIV-1 protease by fullerene derivatives: model building studies and experimental verification.* Journal of the American Chemical Society, 1993. **115**(15): p. 6506-6509.
37. Mueller, N.C. and B. Nowack, *Exposure Modeling of Engineered Nanoparticles in the Environment.* Environmental Science & Technology, 2008. **42**(12): p. 4447-4453.
38. Segawa, Y., H. Ito, and K. Itami, *Structurally uniform and atomically precise carbon nanostructures.* Nature Reviews Materials, 2016. **1**: p. 15002.

39. Upadhyayula, V.K.K., et al., *Application of carbon nanotube technology for removal of contaminants in drinking water: A review.* Science of The Total Environment, 2009. **408**(1): p. 1-13.
40. Zhou, R.W., B. Xu and Y. Li,, *Synthesis, characterization and catalytic properties of CuO nanocrystals with various shapes.* Nanotechnology, 2006.
41. Jang, H.D., Kim, SK. & Kim, SJ., *Effect of Particle Size and Phase Composition of Titanium Dioxide Nanoparticles on the Photocatalytic Properties.* ournal of Nanoparticle Research, 2001.
42. Gupta, A.K. and M. Gupta, *Synthesis and surface engineering of iron oxide nanoparticles for biomedical applications.* Biomaterials, 2005. **26**(18): p. 3995-4021.
43. Larson, D.R., et al., *Water-Soluble Quantum Dots for Multiphoton Fluorescence Imaging in Vivo.* Science, 2003. **300**(5624): p. 1434-1436.
44. Bruchez, M., et al., *Semiconductor Nanocrystals as Fluorescent Biological Labels.* Science, 1998. **281**(5385): p. 2013-2016.
45. Mattoussi, H., et al., *Self-Assembly of CdSe−ZnS Quantum Dot Bioconjugates Using an Engineered Recombinant Protein.* Journal of the American Chemical Society, 2000. **122**(49): p. 12142-12150.
46. Silva, B.F.d., et al., *Analytical chemistry of metallic nanoparticles in natural environments.* TrAC Trends in Analytical Chemistry, 2011. **30**(3): p. 528-540.
47. Shahverdi, A.R., et al., *Synthesis and effect of silver nanoparticles on the antibacterial activity of different antibiotics against Staphylococcus aureus and Escherichia coli.* Nanomedicine: Nanotechnology, Biology and Medicine, 2007. **3**(2): p. 168-171.
48. Benn, T.M. and P. Westerhoff, *Nanoparticle Silver Released into Water from Commercially Available Sock Fabrics.* Environmental Science & Technology, 2008. **42**(11): p. 4133-4139.
49. Sadeghi, B., et al., *Synthesis and characterization of silver nanoparticles for antibacterial activity.* International Journal of Nano Dimension, 2010. **1**(2): p. 119-124.
50. Zhang, X.-D., et al., *Toxicologic effects of gold nanoparticles in vivo by different administration routes.* International journal of nanomedicine, 2010. **5**: p. 771-781.
51. Roney, C., et al., *Targeted nanoparticles for drug delivery through the blood–brain barrier for Alzheimer's disease.* Journal of Controlled Release, 2005. **108**(2): p. 193-214.
52. Schirhagl, R., et al., *Natural and Biomimetic Materials for the Detection of Insulin.* Analytical Chemistry, 2012. **84**(9): p. 3908-3913.
53. Simon, J., E. Flahaut, and M. Golzio, *Overview of Carbon Nanotubes for Biomedical Applications.* Materials (Basel, Switzerland), 2019. **12**(4): p. 624.
54. Jiang, J., J. Pi, and J. Cai, *The Advancing of Zinc Oxide Nanoparticles for Biomedical Applications.* Bioinorganic chemistry and applications, 2018. **2018**: p. 1062562-1062562.
55. Bitar, A., et al., *Silica-based nanoparticles for biomedical applications.* Drug Discovery Today, 2012. **17**(19): p. 1147-1154.
56. Behnam, M.A., et al., *The application of titanium dioxide (TiO(2)) nanoparticles in the photo-thermal therapy of melanoma cancer model.* Iranian journal of basic medical sciences, 2018. **21**(11): p. 1133-1139.
57. Zheng, L., Hong, F., Lu, S. et al., *Effect of nano-TiO2 on strength of naturally aged seeds and growth of spinach.* Biol Trace Elem Res, 2005.

58. Dhall, A. and W. Self, *Cerium Oxide Nanoparticles: A Brief Review of Their Synthesis Methods and Biomedical Applications.* Antioxidants (Basel, Switzerland), 2018. **7**(8): p. 97.
59. Grigore, M.E., et al., *Methods of Synthesis, Properties and Biomedical Applications of CuO Nanoparticles.* Pharmaceuticals (Basel, Switzerland), 2016. **9**(4): p. 75.
60. Hassanpour, P., et al., *Biomedical applications of aluminium oxide nanoparticles.* Micro & Nano Letters, 2018. **13**.
61. Andreescu, S., et al., *Biomedical Applications of Metal Oxide Nanoparticles*, in *Fine Particles in Medicine and Pharmacy*, E. Matijević, Editor. 2012, Springer US: Boston, MA. p. 57-100.
62. Ding, Y., et al., *Relationship between the thermal conductivity and shear viscosity of nanofluids.* Physica Scripta, 2010. **T139**: p. 014078.
63. Arias, L.S., et al., *Iron Oxide Nanoparticles for Biomedical Applications: A Perspective on Synthesis, Drugs, Antimicrobial Activity, and Toxicity.* Antibiotics (Basel, Switzerland), 2018. **7**(2): p. 46.
64. Daniel, S.C.G.K., et al., *Toxicity and immunological activity of silver nanoparticles.* Applied Clay Science, 2010. **48**(4): p. 547-551.
65. Grieger, K.D., et al., *Environmental benefits and risks of zero-valent iron nanoparticles (nZVI) for in situ remediation: Risk mitigation or trade-off?* Journal of Contaminant Hydrology, 2010. **118**(3): p. 165-183.
66. Wu, Y. and S. Hu, *Direct electrochemistry of glucose oxidase in a colloid Au–dihexadecylphosphate composite film and its application to develop a glucose biosensor.* Bioelectrochemistry, 2007. **70**(2): p. 335-341.
67. Robenek, H., *Colloidal gold: Principles, methods, and applications vols. I and II (vol. III in preparation) Edited by M. A. Hayat Academic Press, Inc., New York, 1989 ISBN 0–12–333927–8, Vol. I, 536 pages ISBN 0–12–333928–6, Vol. II, 484 pages.* Scanning, 1990. **12**(4): p. 244-244.
68. S. U. S. Choi, a.J.A.E., *ASME International Mechanical Engineering Congress & Exposition.* Contract W-31-109-ENG-38 of the Energy Technology Division and Materials Science Division, San Francisco, CA, November 12-17, San Francisco, CA, 1995.
69. Rivera-Gil, P., et al., *The Challenge To Relate the Physicochemical Properties of Colloidal Nanoparticles to Their Cytotoxicity.* Accounts of Chemical Research, 2013. **46**(3): p. 743-749.
70. Pelaz, B., et al., *Interfacing Engineered Nanoparticles with Biological Systems: Anticipating Adverse Nano–Bio Interactions.* Small, 2013. **9**(9-10): p. 1573-1584.
71. Feliu, N., et al., *In vivo degeneration and the fate of inorganic nanoparticles.* Chemical Society Reviews, 2016. **45**(9): p. 2440-2457.
72. Parak, W.J., et al., *Biological applications of colloidal nanocrystals.* Nanotechnology, 2003. **14**(7): p. R15-R27.
73. Santos, H.A., ed. *Porous Silicon for Biomedical Applications: Woodhead Publishing series in biomaterials 68*. 2014, Woodhead Publishing Ltd.
74. Fadeel, B., et al., *Bridge over troubled waters: understanding the synthetic and biological identities of engineered nanomaterials.* Wiley Interdisciplinary Reviews: Nanomedicine and Nanobiotechnology, 2013. **5**(2): p. 111-129.
75. Gerion, D., et al., *Synthesis and Properties of Biocompatible Water-Soluble Silica-Coated CdSe/ZnS Semiconductor Quantum Dots.* The Journal of Physical Chemistry B, 2001. **105**(37): p. 8861-8871.

76. Selvan, S.T., et al., *Synthesis of Silica-Coated Semiconductor and Magnetic Quantum Dots and Their Use in the Imaging of Live Cells.* Angewandte Chemie International Edition, 2007. **46**(14): p. 2448-2452.
77. Cedervall, T., et al., *Understanding the nanoparticle–protein corona using methods to quantify exchange rates and affinities of proteins for nanoparticles.* Proceedings of the National Academy of Sciences, 2007. **104**(7): p. 2050.
78. Walkey, C.D. and W.C.W. Chan, *Understanding and controlling the interaction of nanomaterials with proteins in a physiological environment.* Chemical Society Reviews, 2012. **41**(7): p. 2780-2799.
79. Monopoli, M.P., et al., *Biomolecular coronas provide the biological identity of nanosized materials.* Nature Nanotechnology, 2012. **7**: p. 779.
80. Tenzer, S., et al., *Rapid formation of plasma protein corona critically affects nanoparticle pathophysiology.* Nature Nanotechnology, 2013. **8**: p. 772.
81. Xia, X.-R., N.A. Monteiro-Riviere, and J.E. Riviere, *An index for characterization of nanomaterials in biological systems.* Nature Nanotechnology, 2010. **5**(9): p. 671-675.
82. Wan, S., et al., *The "Sweet" Side of the Protein Corona: Effects of Glycosylation on Nanoparticle–Cell Interactions.* ACS Nano, 2015. **9**(2): p. 2157-2166.
83. Hillaireau, H.C., *Nanocarriers' entry into the cell: relevance to drug delivery.* P. Cell. Mol. Life Sci., (2009).
84. Jones, S.W., et al., *Nanoparticle clearance is governed by Th1/Th2 immunity and strain background.* The Journal of Clinical Investigation, 2013. **123**(7): p. 3061-3073.
85. Freund, B., et al., *A Simple and Widely Applicable Method to 59Fe-Radiolabel Monodisperse Superparamagnetic Iron Oxide Nanoparticles for In Vivo Quantification Studies.* ACS Nano, 2012. **6**(8): p. 7318-7325.
86. Moore, A., et al., *Tumoral Distribution of Long-circulating Dextran-coated Iron Oxide Nanoparticles in a Rodent Model.* Radiology, 2000. **214**(2): p. 568-574.
87. Setyawati, M.I., et al., *Understanding and exploiting nanoparticles' intimacy with the blood vessel and blood.* Chemical Society Reviews, 2015. **44**(22): p. 8174-8199.
88. Bargheer, D., et al., *The fate of a designed protein corona on nanoparticles in vitro and in vivo.* Beilstein Journal of Nanotechnology, 2015. **6**: p. 36-46.
89. Bargheer, D., et al., *The distribution and degradation of radiolabeled superparamagnetic iron oxide nanoparticles and quantum dots in mice.* Beilstein Journal of Nanotechnology, 2015. **6**: p. 111-123.
90. Carambia, A., et al., *Nanoparticle-based autoantigen delivery to Treg-inducing liver sinusoidal endothelial cells enables control of autoimmunity in mice.* Journal of Hepatology, 2015. **62**(6): p. 1349-1356.
91. Halamoda-Kenzaoui, B. and S. Bremer-Hoffmann, *Main trends of immune effects triggered by nanomedicines in preclinical studies.* International journal of nanomedicine, 2018. **13**: p. 5419-5431.
92. Bawage, S.S., et al., *Gold nanorods inhibit respiratory syncytial virus by stimulating the innate immune response.* Nanomedicine, 2016. **12**(8): p. 2299-2310.
93. Rabolli, V., et al., *The alarmin IL-1alpha is a master cytokine in acute lung inflammation induced by silica micro- and nanoparticles.* Part Fibre Toxicol, 2014. **11**: p. 69.

94. Ng, C.-T., et al., *Inflammatory changes in lung tissues associated with altered inflammation-related microRNA expression after intravenous administration of gold nanoparticles in vivo.* ACS Biomaterials Science & Engineering, 2016. **2**(11): p. 1959-1967.
95. Zhang, X.D., et al., *In vivo renal clearance, biodistribution, toxicity of gold nanoclusters.* Biomaterials, 2012. **33**(18): p. 4628-38.
96. Cho, Y.C., et al., *In vitro and in vivo comparison of the immunotoxicity of single- and multi-layered graphene oxides with or without pluronic F-127.* Sci Rep, 2016. **6**: p. 38884.
97. Erf, G.F., et al., *T lymphocytes dominate local leukocyte infiltration in response to intradermal injection of functionalized graphene-based nanomaterial.* J Appl Toxicol, 2017. **37**(11): p. 1317-1324.
98. Del Campo, J.A., P. Gallego, and L. Grande, *Role of inflammatory response in liver diseases: Therapeutic strategies.* World journal of hepatology, 2018. **10**(1): p. 1-7.
99. Ludwig, J., et al., *Nonalcoholic steatohepatitis: Mayo Clinic experiences with a hitherto unnamed disease.* Mayo Clin Proc, 1980. **55**(7): p. 434-8.
100. Buzzetti, E., M. Pinzani, and E.A. Tsochatzis, *The multiple-hit pathogenesis of non-alcoholic fatty liver disease (NAFLD).* Metabolism, 2016. **65**(8): p. 1038-48.
101. Begriche, K., et al., *Mitochondrial adaptations and dysfunctions in nonalcoholic fatty liver disease.* Hepatology, 2013. **58**(4): p. 1497-507.
102. Bayliss, S.C., et al., *The culture of mammalian cells on nanostructured silicon.* Advanced Materials, 1999. **11**(4): p. 318-321.
103. Canham, L.T., *Bioactive silicon structure fabrication through nanoetching techniques.* Advanced Materials, 1995. **7**(12): p. 1033-1037.
104. Salonen, J., et al., *Mesoporous silicon in drug delivery applications.* Journal of pharmaceutical sciences, 2008. **97**(2): p. 632-653.
105. Sailor, M.J., *Fundamentals of Porous Silicon Preparation*, in *Porous Silicon in Practice*. 2012. p. 1-42.
106. Jarvis, K.L., T.J. Barnes, and C.A. Prestidge, *Surface chemistry of porous silicon and implications for drug encapsulation and delivery applications.* Advances in Colloid and Interface Science, 2012. **175**: p. 25-38.
107. Herino, R., et al., *Porosity and pore size distributions of porous silicon layers.* Journal of the electrochemical society, 1987. **134**(8): p. 1994-2000.
108. Riikonen, J., et al., *Systematic in vitro and in vivo study on porous silicon to improve the oral bioavailability of celecoxib.* Biomaterials, 2015. **52**: p. 44-55.
109. Li, W., et al., *Tailoring Porous Silicon for Biomedical Applications: From Drug Delivery to Cancer Immunotherapy.* Advanced Materials, 2018. **30**(24): p. 1703740.
110. Anderson, S.H.C., et al., *Dissolution of different forms of partially porous silicon wafers under simulated physiological conditions.* physica status solidi (a), 2003. **197**(2): p. 331-335.
111. Santos, H.A., et al., *In vitro cytotoxicity of porous silicon microparticles: Effect of the particle concentration, surface chemistry and size.* Acta Biomaterialia, 2010. **6**(7): p. 2721-2731.
112. Bley, R.A., et al., *Characterization of Silicon Nanoparticles Prepared from Porous Silicon.* Chemistry of Materials, 1996. **8**(8): p. 1881-1888.

113. Roberts, D.S., et al., *Preparation of Photoluminescent Porous Silicon Nanoparticles by High-Pressure Microfluidization.* Particle & Particle Systems Characterization, 2017. **34**(3): p. 1600326.
114. Lam, C., et al., *Large-scale synthesis of ultrafine Si nanoparticles by ball milling.* Journal of Crystal Growth, 2000. **220**(4): p. 466-470.
115. Silva, A.C., et al., *Preparation, characterization and biocompatibility studies on risperidone-loaded solid lipid nanoparticles (SLN): High pressure homogenization versus ultrasound.* Colloids and Surfaces B: Biointerfaces, 2011. **86**(1): p. 158-165.
116. Dai, F., et al., *Bottom-up synthesis of high surface area mesoporous crystalline silicon and evaluation of its hydrogen evolution performance.* Nature Communications, 2014. **5**(1): p. 3605.
117. Foraker, A.B., et al., *Microfabricated porous silicon particles enhance paracellular delivery of insulin across intestinal Caco-2 cell monolayers.* Pharmaceutical research, 2003. **20**(1): p. 110-116.
118. Vaccari, L., et al., *Porous silicon as drug carrier for controlled delivery of doxorubicin anticancer agent.* Microelectronic Engineering, 2006. **83**(4): p. 1598-1601.
119. Q. Shabir, K.W., D. K. Nadarassan, A. Loni, L. T. Canham, M. Terracciano, L. De Stefano, I., *Quantification and Reduction of the Residual Chemical Reactivity of Passivated Biodegradable Porous Silicon for Drug Delivery Applications.* Springer Netherlands, 2017.
120. Haidary, S.M., et al., *Nanoporous silicon as drug delivery systems for cancer therapies.* J. Nanomaterials, 2012. **2012**: p. 1-15.
121. Pap, A.E., et al., *Thermal oxidation of porous silicon: Study on structure.* Applied Physics Letters, 2005. **86**(4): p. 041501.
122. Loni, A., et al., *Chemical Oxidation of Porous Silicon in Alcohol-Lye Solutions.* ECS Journal of Solid State Science and Technology, 2015. **4**(5): p. P149-P151.
123. Jarvis, K.L., T.J. Barnes, and C.A. Prestidge, *Aqueous and Thermal Oxidation of Porous Silicon Microparticles: Implications on Molecular Interactions.* Langmuir, 2008. **24**(24): p. 14222-14226.
124. Wang, J.-F., J.-S. Chen, and Z.-F. Zhou, *Preparation of Porous Silicon by Sodiothermic Reduction of Zeolite and Photoactivation for Benzene Oxidation.* European Journal of Inorganic Chemistry, 2015. **2015**(8): p. 1330-1333.
125. Cao, D.T., L.T.Q. Ngan, and C.T. Anh, *Enhancement and stabilization of the photoluminescence from porous silicon prepared by Ag-assisted electrochemical etching.* Surface and Interface Analysis, 2013. **45**(3): p. 762-766.
126. E. Bateman, J., et al., *Rôle for organic molecules in the oxidation of porous silicon.* Chemical Communications, 1997(23): p. 2275-2276.
127. Salonen, J., et al., *Stabilization of porous silicon surface by thermal decomposition of acetylene.* Applied Surface Science, 2004. **225**(1): p. 389-394.
128. Mäkilä, E., et al., *Amine Modification of Thermally Carbonized Porous Silicon with Silane Coupling Chemistry.* Langmuir, 2012. **28**(39): p. 14045-14054.
129. Björkqvist, M., J. Salonen, and E. Laine, *Humidity behavior of thermally carbonized porous silicon.* Applied Surface Science, 2004. **222**(1): p. 269-274.
130. Wang, C.-F., *Chemical surface modification of porous silicon nanoparticles for cancer therapy.* Helsingin yliopisto, 2015.
131. Buriak, J.M., M.P. Stewart, and M.J. Allen, *Functionalization of Porous Silicon Surfaces through Hydrosilylation Reactions.* MRS Proceedings, 1998. **536**: p. 173.

132. Boukherroub, R., et al., *Thermal Hydrosilylation of Undecylenic Acid with Porous Silicon.* Journal of The Electrochemical Society, 2002. **149**(2): p. H59-H63.
133. Kovalev, D., et al., *Photodegradation of porous silicon induced by photogenerated singlet oxygen molecules.* Applied Physics Letters, 2004. **85**(16): p. 3590-3592.
134. Low, S.P., et al., *Generation of reactive oxygen species from porous silicon microparticles in cell culture medium.* Journal of Biomedical Materials Research Part A, 2010. **93A**(3): p. 1124-1131.
135. Alhmoud, H., et al., *Porous Silicon Nanodiscs for Targeted Drug Delivery.* Advanced Functional Materials, 2015. **25**(7): p. 1137-1145.
136. De Angelis, F., et al., *Water soluble nanoporous nanoparticle for in vivo targeted drug delivery and controlled release in B cells tumor context.* Nanoscale, 2010. **2**(10): p. 2230-2236.
137. Croissant, J.G., Y. Fatieiev, and N.M. Khashab, *Degradability and Clearance of Silicon, Organosilica, Silsesquioxane, Silica Mixed Oxide, and Mesoporous Silica Nanoparticles.* Advanced Materials, 2017. **29**(9): p. 1604634.
138. Tzur-Balter, A., et al., *Mechanism of erosion of nanostructured porous silicon drug carriers in neoplastic tissues.* Nature Communications, 2015. **6**(1): p. 6208.
139. Wu, E.C., et al., *Real-time monitoring of sustained drug release using the optical properties of porous silicon photonic crystal particles.* Biomaterials, 2011. **32**(7): p. 1957-1966.
140. Cheung, A.S. and D.J. Mooney, *Engineered materials for cancer immunotherapy.* Nano Today, 2015. **10**(4): p. 511-531.
141. Ainslie, K.M., et al., *In vitro Immunogenicity of Silicon-Based Micro- and Nanostructured Surfaces.* ACS Nano, 2008. **2**(5): p. 1076-1084.
142. Meraz, I.M., et al., *Activation of the Inflammasome and Enhanced Migration of Microparticle-Stimulated Dendritic Cells to the Draining Lymph Node.* Molecular Pharmaceutics, 2012. **9**(7): p. 2049-2062.
143. Godin, B., et al., *Multistage Mesoporous Silicon-based Nanocarriers: Biocompatibility with Immune Cells and Controlled Degradation in Physiological Fluids.* Controll Release Newsl, 2008. **25**(4): p. 9-11.
144. Shahbazi, M.-A., et al., *Surface chemistry dependent immunostimulative potential of porous silicon nanoplatforms.* Biomaterials, 2014. **35**(33): p. 9224-9235.
145. Kakizawa, Y., et al., *Precise manipulation of biophysical particle parameters enables control of proinflammatory cytokine production in presence of TLR 3 and 4 ligands.* Acta Biomaterialia, 2017. **57**: p. 136-145.
146. Shima, F., T. Akagi, and M. Akashi, *Effect of Hydrophobic Side Chains in the Induction of Immune Responses by Nanoparticle Adjuvants Consisting of Amphiphilic Poly(γ-glutamic acid).* Bioconjugate Chemistry, 2015. **26**(5): p. 890-898.
147. Jurkić, L.M., et al., *Biological and therapeutic effects of ortho-silicic acid and some ortho-silicic acid-releasing compounds: New perspectives for therapy.* Nutrition & Metabolism, 2013. **10**(1): p. 2.
148. Salonen, J., et al., *Mesoporous silicon microparticles for oral drug delivery: loading and release of five model drugs.* J Control Release, 2005. **108**(2-3): p. 362-74.

149. Bimbo, L.M., et al., *Inhibition of influenza A virus infection in vitro by saliphenylhalamide-loaded porous silicon nanoparticles.* ACS Nano, 2013. **7**(8): p. 6884-93.
150. Park, J.S., et al., *Cisplatin-loaded porous Si microparticles capped by electroless deposition of platinum.* Small (Weinheim an der Bergstrasse, Germany), 2011. **7**(14): p. 2061-2069.
151. De Rosa, E., et al., *Agarose surface coating influences intracellular accumulation and enhances payload stability of a nano-delivery system.* Pharm Res, 2011. **28**(7): p. 1520-30.
152. Shrestha, N., et al., *Chitosan-modified porous silicon microparticles for enhanced permeability of insulin across intestinal cell monolayers.* Biomaterials, 2014. **35**(25): p. 7172-9.
153. De Stefano, L., et al., *Oligonucleotides direct synthesis on porous silicon chip.* Nucleic Acids Symp Ser (Oxf), 2008(52): p. 721-2.
154. McClorey, G. and S. Banerjee, *Cell-Penetrating Peptides to Enhance Delivery of Oligonucleotide-Based Therapeutics.* Biomedicines, 2018. **6**(2): p. 51.
155. McInnes, S.J. and N.H. Voelcker, *Porous silicon-based nanostructured microparticles as degradable supports for solid-phase synthesis and release of oligonucleotides.* Nanoscale Res Lett, 2012. **7**(1): p. 385.
156. Wan, Y., et al., *Cancer-targeting siRNA delivery from porous silicon nanoparticles.* Nanomedicine, 2014. **9**(15): p. 2309-2321.
157. Freytag, L.C. and J.D. Clements, *Chapter 61 - Mucosal Adjuvants: New Developments and Challenges*, in *Mucosal Immunology (Fourth Edition)*, J. Mestecky, et al., Editors. 2015, Academic Press: Boston. p. 1183-1199.
158. Gu, L., et al., *Multivalent porous silicon nanoparticles enhance the immune activation potency of agonistic CD40 antibody.* Advanced materials (Deerfield Beach, Fla.), 2012. **24**(29): p. 3981-3987.
159. Grewal, I.S. and R.A. Flavell, *CD40 AND CD154 IN CELL-MEDIATED IMMUNITY.* Annual Review of Immunology, 1998. **16**(1): p. 111-135.
160. Makidon, P.E., et al., *Induction of immune response to the 17 kDa OMPA Burkholderia cenocepacia polypeptide and protection against pulmonary infection in mice after nasal vaccination with an OMP nanoemulsion-based vaccine.* Med Microbiol Immunol, 2010. **199**(2): p. 81-92.
161. Shen, H., et al., *Enhanced and prolonged cross-presentation following endosomal escape of exogenous antigens encapsulated in biodegradable nanoparticles.* Immunology, 2006. **117**(1): p. 78-88.
162. Demento, S.L., et al., *Inflammasome-activating nanoparticles as modular systems for optimizing vaccine efficacy.* Vaccine, 2009. **27**(23): p. 3013-21.
163. Moon, J.J., et al., *Interbilayer-crosslinked multilamellar vesicles as synthetic vaccines for potent humoral and cellular immune responses.* Nature materials, 2011. **10**(3): p. 243-251.
164. Peek, L.J., C.R. Middaugh, and C. Berkland, *Nanotechnology in vaccine delivery.* Advanced drug delivery reviews, 2008. **60**(8): p. 915-928.
165. Gu, L., et al., *In vivo time-gated fluorescence imaging with biodegradable luminescent porous silicon nanoparticles.* Nat Commun, 2013. **4**: p. 2326.
166. Leblond, F., et al., *Pre-clinical whole-body fluorescence imaging: Review of instruments, methods and applications.* Journal of Photochemistry and Photobiology B: Biology, 2010. **98**(1): p. 77-94.
167. Park, J.H., et al., *Biodegradable luminescent porous silicon nanoparticles for in vivo applications.* Nat Mater, 2009. **8**(4): p. 331-6.

168. Secret, E., et al., *Anionic porphyrin-grafted porous silicon nanoparticles for photodynamic therapy.* Chemical Communications, 2013. **49**(39): p. 4202-4204.
169. Osminkina, L.A., et al., *Photoluminescent biocompatible silicon nanoparticles for cancer theranostic applications.* J Biophotonics, 2012. **5**(7): p. 529-35.
170. Joo, J., et al., *Gated Luminescence Imaging of Silicon Nanoparticles.* ACS Nano, 2015. **9**(6): p. 6233-6241.
171. Gongalsky, M.B., et al., *Enhanced photoluminescence of porous silicon nanoparticles coated by bioresorbable polymers.* Nanoscale Research Letters, 2012. **7**(1): p. 446.
172. Secret, E., et al., *Two-Photon Excitation of Porphyrin-Functionalized Porous Silicon Nanoparticles for Photodynamic Therapy.* Advanced Materials, 2014. **26**(45): p. 7643-7648.
173. Chouikrat, R., et al., *Non Polymeric Nanoparticles for Photodynamic Therapy Applications: Recent Developments.* Current Medicinal Chemistry, 2012. **19**(6): p. 781-792.
174. Hong, C. and C. Lee, *In vitro cell tests of pancreatic malignant tumor cells by photothermotherapy based on DMSO porous silicon colloids.* Lasers in Medical Science, 2014. **29**(1): p. 221-223.
175. Hong, C., et al., *Porous silicon nanoparticles for cancer photothermotherapy.* Nanoscale Res Lett, 2011. **6**(1): p. 321.
176. Yokoi, K., et al., *Porous silicon nanocarriers for dual targeting tumor associated endothelial cells and macrophages in stroma of orthotopic human pancreatic cancers.* Cancer Letters, 2013. **334**(2): p. 319-327.
177. Decuzzi, P., et al., *Size and shape effects in the biodistribution of intravascularly injected particles.* Journal of Controlled Release, 2010. **141**(3): p. 320-327.
178. Bimbo, L.M., et al., *Biocompatibility of Thermally Hydrocarbonized Porous Silicon Nanoparticles and their Biodistribution in Rats.* ACS Nano, 2010. **4**(6): p. 3023-3032.
179. Jalkanen, T., et al., *Thermally promoted addition of undecylenic acid on thermally hydrocarbonized porous silicon optical reflectors.* Nanoscale Research Letters, 2012. **7**(1): p. 311.
180. Salonen, J., E. Laine, and L. Niinistö, *Thermal carbonization of porous silicon surface by acetylene.* Journal of Applied Physics, 2002. **91**(1): p. 456-461.
181. Liu, D., et al., *Microfluidic assisted one-step fabrication of porous silicon@acetalated dextran nanocomposites for precisely controlled combination chemotherapy.* Biomaterials, 2015. **39**: p. 249-59.
182. Brunauer, S. and L. Copeland. *Physical adsorption of gases and vapors on solids*. in *Symposium on Properties of Surfaces*. 1963. ASTM International.
183. Salonen, J., V.-P. Lehto, and E. Laine, *Thermal oxidation of free-standing porous silicon films.* Applied Physics Letters, 1997. **70**(5): p. 637-639.
184. Fan, F., et al., *Pharmacological targeting of kinases MST1 and MST2 augments tissue repair and regeneration.* Sci Transl Med, 2016. **8**(352): p. 352ra108.
185. Antoniades, C.G., et al., *The importance of immune dysfunction in determining outcome in acute liver failure.* J Hepatol, 2008. **49**(5): p. 845-61.
186. Gowda, S., et al., *A review on laboratory liver function tests.* The Pan African medical journal, 2009. **3**: p. 17-17.
187. Giannini, E., et al., *Progressive Liver Functional Impairment Is Associated with an Increase in AST/ALT Ratio.* Digestive Diseases and Sciences, 1999. **44**(6): p. 1249-1253.

188. Altomare, E., G. Vendemiale, and O. Albano, *Hepatic glutathione content in patients with alcoholic and non alcoholic liver diseases.* Life Sciences, 1988. **43**(12): p. 991-998.
189. Wu, Z., et al., *Acute liver failure: mechanisms of immune-mediated liver injury.* Liver Int, 2010. **30**(6): p. 782-94.
190. Kowaltowski, A.J. and A.E. Vercesi, *Mitochondrial damage induced by conditions of oxidative stress.* Free Radic Biol Med, 1999. **26**(3-4): p. 463-71.
191. Limnell, T., et al., *Surface chemistry and pore size affect carrier properties of mesoporous silicon microparticles.* International Journal of Pharmaceutics, 2007. **343**(1): p. 141-147.
192. Shahbazi, M.A., et al., *The mechanisms of surface chemistry effects of mesoporous silicon nanoparticles on immunotoxicity and biocompatibility.* Biomaterials, 2013. **34**(31): p. 7776-89.
193. Liu, Z., et al., *Multifunctional Nanohybrid Based on Porous Silicon Nanoparticles, Gold Nanoparticles, and Acetalated Dextran for Liver Regeneration and Acute Liver Failure Theranostics.* Adv Mater, 2018. **30**(24): p. e1703393.
194. Tanaka, T., et al., *In vivo evaluation of safety of nanoporous silicon carriers following single and multiple dose intravenous administrations in mice.* Int J Pharm, 2010. **402**(1-2): p. 190-7.